Best Available
Copy
for all Pictures

AD/A-003 330

TUBULAR COMPOSITE HLH ROTOR BLADE SECTION

Sam Yao, et al

Fiber Science, Incorporated

Prepared for:

Army Air Mobility Research and Development Laboratory

November 1974

DISTRIBUTED BY:

NTIS
National Technical Information Service
U. S. DEPARTMENT OF COMMERCE

Unclassified

SECURITY CLASSIFICATION OF THIS PAGE (When Data Entered)

REPORT DOCUMENTATION PAGE

READ INSTRUCTIONS BEFORE COMPLETING FORM

1. REPORT NUMBER USAAMRDL-TR-74-95 / 2. GOVT ACCESSION NO.	3. RECIPIENT'S CATALOG NUMBER AD/A-003330
4. TITLE (and Subtitle) TUBULAR COMPOSITE HLH ROTOR BLADE SECTION	5. TYPE OF REPORT & PERIOD COVERED Final November 1972 - December 1973
	6. PERFORMING ORG. REPORT NUMBER
7. AUTHOR(s) Sam Yao, Dale Abildskov	8. CONTRACT OR GRANT NUMBER(s) DAAJ02-73-C-0025
9. PERFORMING ORGANIZATION NAME AND ADDRESS Fiber Science, Inc. Gardena, Calif. 90248	10. PROGRAM ELEMENT, PROJECT, TASK AREA & WORK UNIT NUMBERS Project 1X263203D156
11. CONTROLLING OFFICE NAME AND ADDRESS Eustis Directorate, U. S. Army Air Mobility Research and Development Laboratory Fort Eustis, Va. 23604	12. REPORT DATE November 1974
	13. NUMBER OF PAGES
14. MONITORING AGENCY NAME & ADDRESS(if different from Controlling Office)	15. SECURITY CLASS. (of this report) Unclassified
	15a. DECLASSIFICATION/DOWNGRADING SCHEDULE

16. DISTRIBUTION STATEMENT (of this Report)

Approved for public release; distribution unlimited.

17. DISTRIBUTION STATEMENT (of the abstract entered in Block 20, if different from Report)

18. SUPPLEMENTARY NOTES

19. KEY WORDS (Continue on reverse side if necessary and identify by block number)

Composite materials
Rotor blades
Tubes
Heavy-lift helicopter

20. ABSTRACT (Continue on reverse side if necessary and identify by block number)

This report describes the results of a research and development program to design, analyze, and fabricate a 16-foot-long section, including the root end attachment, of an HLH size rotor blade. The design of the blade section was based upon the tubular-reinforced-composite wet filament wound concept.

The blade design and the fabrication techniques developed are new and can be applicable to low-cost automated composite helicopter rotor blade fabrication. Fibrous materials used in the blade include S-Glass, Kevlar 49, and Thornel 300 graphite, all of which were held by an epoxy resin matrix. All

DD FORM 1 JAN 73 1473 EDITION OF 1 NOV 65 IS OBSOLETE

Unclassified

SECURITY CLASSIFICATION OF THIS PAGE (When Data Entered)

Block 20. Abstract - continued

winding was done wet. The cost of raw materials was kept at a minimum by using the higher priced graphite only in those areas where it afforded the greatest advantage.

A technique was developed for handling the wet skin material without distorting the fiber orientation while it was transported from the winding machine into the forming mold. This process makes it possible to handle full-length blades involving considerable weights of uncured, wound material.

It was found that unidirectional graphite material could be wound onto the upper and lower sides of the main spar tubes more easily than anticipated, making the tube fabrication a relatively simple procedure.

All mandrels used in the program were air-inflated thermoplastic. They offered many fabrication and cost advantages over hard mandrels. The plastic air-inflated mandrels were in fact so successful that even if unlimited funds were available for high-quantity production tooling, they would now be chosen over hard tooling.

EUSTIS DIRECTORATE POSITION STATEMENT

This report has been reviewed by the Eustis Directorate, U. S. Army Air Mobility Research and Development Laboratory and is considered to be technically sound.

The research program provides technology for the fabrication of HLH size main rotor blades utilizing wet-filament-winding techniques in conjunction with multi-tubular spar concepts. A unique root end attachment technique in which the end fittings are integrally wound as part of the spar tubular elements was developed. The results provide a base technology for the development of highly tailorable composite main rotor blades.

The technical monitor was Mr. I. E. Figge, Sr., Technology Applications Division.

DISCLAIMERS

The findings in this report are not to be construed as an official Department of the Army position unless so designated by other authorized documents.

When Government drawings, specifications, or other data are used for any purpose other than in connection with a definitely related Government procurement operation, the United States Government thereby incurs no responsibility nor any obligation whatsoever; and the fact that the Government may have formulated, furnished, or in any way supplied the said drawings, specifications, or other data is not to be regarded by implication or otherwise as in any manner licensing the holder or any other person or corporation, or conveying any rights or permission, to manufacture, use, or sell any patented invention that may in any way be related thereto.

Trade names cited in this report do not constitute an official endorsement or approval of the use of such commercial hardware or software.

DISPOSITION INSTRUCTIONS

Destroy this report when no longer needed. Do not return it to the originator.

PREFACE

This report was prepared by Fiber Science, Inc., a subsidiary of the Edo Corporation, in accordance with Contract DAAJ02-73-C-0025 (DA Project 1X263203D156), issued by the Eustis Directorate, U. S. Army Air Mobility Research and Development Laboratory, Fort Eustis, Virginia. Mr. I. E. Figge, Sr., was the U. S. Army program technical monitor.

The activities reported herein cover the period from November 1972 to December 1973. The FSI Project Engineer was Mr. David Wall.

TABLE OF CONTENTS

Preceding page blank

LIST OF ILLUSTRATIONS

LIST OF TABLES

INTRODUCTION

Helicopter rotor blades fabricated from advanced composite materials offer advantages over metallic blades by providing longer blade life, making repairs easier, giving ballistic tolerance, and reducing radar cross section. An additional advantage of reduced cost is obtained by the use of a wet-filament-winding process using raw materials at their lowest possible cost level, and minimizing hand labor by the use of automated winding machines.

During this program, a 16-foot-long section, including the root end attachment fitting, of an HLH rotor blade (40-inch chord, 486-inch span) was designed and fabricated using filament-wound tubular elements, unidirectional (longos) nose material, and skin material as the main structural elements.

Figures 1 and 2 show the completed blade section and cross section of the blade respectively. Table 1 summarizes the criteria and design cross-sectional properties of the tubular composite blade from Station 138 to Station 258.

BLADE DESIGN

GENERAL CONFIGURATION

A blade section was designed and fabricated to the general configuration delineated in Figure 3. The external geometry and attachment are identical to those of the Boeing Company's HLH rotor blade except that an NACA 0015 airfoil was used versus an NACA 43015 to simplify the tooling. Figure 4 shows the two airfoil shapes.

DESIGN CRITERIA

The design goal was to match the geometry, stiffness, strength, center of gravity, and dynamic characteristics of the Boeing Company's HLH blade using FSI's tubular composite blade design and the wet-filament-winding process.

Figure 3 shows the blade stations and overall dimensions.

The average blade cross-sectional properties, taken from Boeing Company data, from Station 138.00 to Station 258.00 are as follows:

$$W = 1.60 \text{ lb/in.}$$
$$CG = 10.44 \text{ in.}$$
$$EA = 112 \times 10^6 \text{ lb}$$
$$EIX = 385 \times 10^6 \text{ lb-in.}^2$$
$$EIY = 9000 \times 10^6 \text{ lb-in.}^2$$
$$GJ = 255 \times 10^6 \text{ lb-in.}^2$$

The loading data from the Boeing Company HLH data is shown in Figures 5 through 9.

The design centrifugal force (CF) load at Station 26 is 150,000 pounds (156 rpm). The limit rotor speed is 177 rpm, and the ultimate CF load is to be taken at 1.5 times limit.

The fatigue consideration is:

3600 hours life - 1.2 x high-speed level flight (156 rpm)
(Mean - 3σ) for material allowable

200 hours life - After detectable damage
(Mean - 2σ) for material allowable

PRELIMINARY DESIGN

Twelve configurations were studied during the preliminary design phase of the program (see Figures 10 through 21). The properties of these configurations are summarized in Table 2. Configuration 12A was selected for fabrication.

COMPONENT DESIGN

The fibers and resin were selected in accordance with the structural requirements at the lowest material cost. Candidate materials studied in the program are shown in Tables 3, 4, and 5. The materials, volume fraction, winding angles, etc., selected for the various blade components are presented in Table 6.

The design philosophy behind each subcomponent of the rotor blade (see Figure 22) and the design techniques contributing to the final configuration are discussed below.

Skin

The outside skin was made up of four layers of Kevlar 49/epoxy helically wound at ±40 degrees to the spanwise axis. The inside skin consisted of one ply of Style 1557 E-Glass fabric/epoxy. A .25-inch-thick piece of 4 lb/ft^3 density PVC foam (Rigicell 400) separated the inner and outer skins. The PVC foam was terminated at each of the tubular elements (spars) in order to make a direct shear transfer from the tubes to both skins. The purpose of making the skin a sandwich wall construction was to enable it to transmit the aerodynamic (air pressure) loads to the tubular spar elements. The limit airload pressure distribution ranges from 12 psi at .35 chord to zero at the trailing edge.

Nose Longos

The nose longo material (unidirectional S-Glass/epoxy) serves a primary function as balance weight for control of the cg location and a secondary function of adding to the strength and stiffness of the blade. The fibers are wrapped around the root end fitting, thus making a direct attachment to the fitting.

Tubes 1, 2, and 3

These tubes collectively form the spar of the blade. They carry the major portion of the beamwise shear loading and approximately 31% of the torsional loading. Incorporated in the upper and lower regions of tubes 2 and 3 are unidirectional graphite windings that extend the full length of the blade. This graphite material accounts for approximately 58.6% of the blade's beamwise stiffness and 30.3% of its spanwise stiffness. The unidirectional graphite material wraps around a metallic fitting inside the wound tube, which in turn transfers any tube loads into the main root end fitting.

The tubes are filament-wound S-Glass epoxy having 80% of the fibers oriented at ±30 degrees to the spanwise direction and % of the windings in the circumferential (hoop) direction. The undirectional graphite material is interspersed between helical and hoop layers to maximize shear area and to increase impact resistance of the graphite material.

Tubes 4, 5, and 6

These tubes, working in conjunction with the skin, transmit the airloads on the aft portion of the blade to the spar. The skin carries the moment and the tubes carry the shear (see Figure 23). The tubes were made using a sandwich wall construction to minimize their weights. The tube core thickness, density, strength, and facing properties were based on loading requirements. Conservatively, the truss action of the skin and the tubes' spanwise shear strengrh and stiffness were neglected in the sizing analysis of the tubes.

Attachment Fitting

The root end fitting is designed to attach to the helicopter rotor hub using two pins, similar to the Boeing Company's HLH blade. It consists of an aluminum block into which the three spar tubes are bonded and pinned, and around which the nose longo material is wrapped. The skin and skin doubler material feed their loads into the two attaching pins through steel sheets that are laminated between plies. The steel sheets were necessary because of the low bearing and shear allowables of the composite material.

The fitting used does not represent flight-weight hardware.

STIFFNESS CALCULATIONS

The cross-sectional properties (center of gravity, weight, and stiffness) were calculated by a computer program. Figure 24 and Table 7 show the basic blade cross section and the computer output. It must be noted that the densities used by the computer were modified to include the effects of adhesive as well as the component weights.

BLADE FABRICATION

The tubular composite rotor blade was primarily fabricated using a combination of wet-filament-winding, molding, and laminating techniques.

The major tasks of fabrication were:

1. Filament-winding tubular elements.
2. Filament-winding and molding nose longos.
3. Machining of root end fitting.
4. Assembly of tubular elements to root end fitting.
5. Filament-winding and molding of outside skin.
6. Laminating and assembly of inside skin and core to outside skin.
7. Assembly of tubular elements and skin.
8. Winding and laminating doubler material in the blade root end transition area.
9. Laminating inboard closing rib.

Task 1. The tubular elements were fabricated by wet filament winding over plastic air-inflated mandrels to the desired thickness. The mandrels were .05-inch-thick cellulose acetate and were pressurized from 2 to 30 psig (pressure was increased as winding progressed) during the winding operation. All tubular elements were cured as a group in the root end fitting while supported in the skin mold to insure fit and straightness (see Figures 25 through 30).

Task 2. The nose longo material was wet-wound around two spools, one simulating the root end fitting. While still in the uncured condition, the windings were weighed and excess resin was removed until the proper weight was obtained; at that time, it was configurated in a mold, pretensioned, and cured. Figure 31 shows the skin (main) and nose longo molds.

Task 3. The root end fitting was machined from a solid block of aluminum (see Figures 32 and 33).

Task 4. The tubular elements, while still in the uncured condition, and the nose longo material were attached to the root end fitting and bonded to one another while being supported by the skin mold (see Figures 34 through 36). Shims were used in the mold to represent the skin thickness in order to insure a proper fit when assembled with the skin.

Task 5. The outside skin was fabricated by w t filament winding over a 20-inch-diameter by 17-foot-long air-inflated plastic mandrel to the desired thickness. The mandrel (see Figure 37) was fabricated from .09-inch-thick styrene sheets with butt joints held together with adhesive tape. Wooden bulkheads were used to support the ends of the plastic mandrel. Inside the mandrel was a support structure that was used to support and configure the wet-wound material while being placed into the skin mold (see Figure 38). The skin material was fabricated twice before a suitable technique was found for handling and bagging it to the mold. Initial handling techniques tried were to position the wound material over the mold and gradually deflate the inside bag, allowing the skin material to settle into the mold (see Figure 39). The principal problem with this technique was getting sufficient material up into the nose of the mold. This problem was overcome with the support tooling inside the mandrel, which pushed the material up into the nose and simplified the transferring of the material into the mold. During the winding operation the pressure inside the mandrel ranged from .2 to 10 psi.

Figure 40 shows the wound skin material.

Task 7. The assembly of the tubes, nose balance, and root end fitting with the precured sandwich wall skin was made using the skin main mold to support the assembly while the adhesive was cured. Figure 41 shows the layup of the inside skin and core material.

Task 8. Doubler material was wet-wound over air-inflated plastic mandrels using essentially the same process as the skin material (see Figure 42). This material, while still in the uncured condition, was cut with scissors and removed from the mandrel. It was then laid up by hand along with steel sheets in the fitting area and vacuum bag cured (see Figure 43).

Task 9. The inboard closing rib was fabricated from glass fabric/epoxy. First the tube ends were bonded to a precured glass fabric/epoxy rib, which was then configurated to the shape of the airfoil. Over this rib, layers of glass fabric/epoxy were laid, which tied the rib to the outside skin surface.

COST ANALYSIS

The cost estimate for the production of tubular composite HLH rotor blades is shown below. This estimate is based on a quantity of 4,000 blades, and the base is on the 2,000th blade. The following rates are the estimated 1973 level for production-oriented shops:

Shop Labor	$4.75/hour
Quality Control Labor	$6.00/hour

DIRECT MATERIAL COSTS

1.	Purchased parts (root end fitting)		$ 500.00
2.	Raw materials		8,000.00
3.	Subcontracted items - balancing system materials, leading-edge strip, painting		1,000.00
		Total Materials	$9,500.00
4.	Material burden - 10%		950.00
		Net Materials	$10,450.00

LABOR

	Hours	
Winding		
Tubes	144	
Nose Longos	16	
Skin	24	
Reinforcing materials	32	
Molding		
Nose longos	24	
Skin	96	
Laminating		
Ribs	32	
Root end reinforcing	48	
Assembly	240	
Leading-edge protection	24	
Trim and cleanup	32	
Balancing	32	
	744	$3,534.00
Quality assurance	144	864.00
Total manufacturing labor		$4,398.00

OVERHEAD

As applied to labor - 120% for a production-oriented shop

($4,398.00 x 120%) =

Total direct cost	$5,277.00

GENERAL AND ADMINISTRATIVE

As applied to direct cost - 20% for a production-oriented shop

($20,125.00 x 20%) =	$4,025.00
TOTAL COST PER BLADE	$24,150.00

CONCLUDING REMARKS

1. A tubular composite HLH size rotor blade can be fabricated by the wet-filament-winding process.

2. A method of wet filament winding over a large air-inflated flexible plastic membrane which can later be deformed into the shape of an airfoil without causing the fibers to become mislocated was demonstrated.

3. A method was developed for handling and positioning in a mold large filament-wound tubular elements that are uncured.

4. The process of winding longo material interspersed with helical windings was demonstrated. The process proved to be much easier than anticipated.

5. A new method of attaching tubular elements to a root end fitting was conceived and demonstrated. One root end section of an HLH size blade was successfully fabricated.

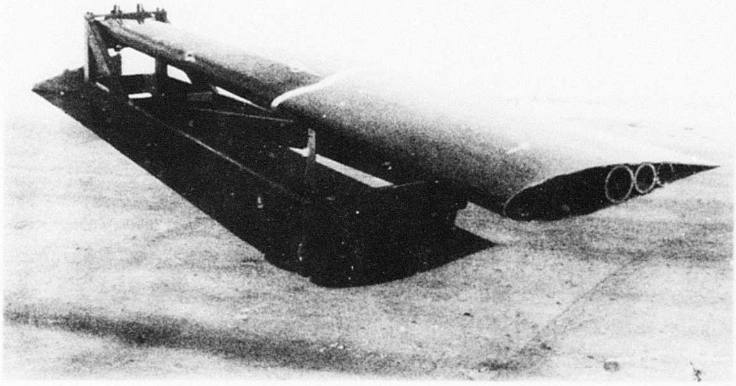

Figure 1. Completed tubular composite HLH size blade section.

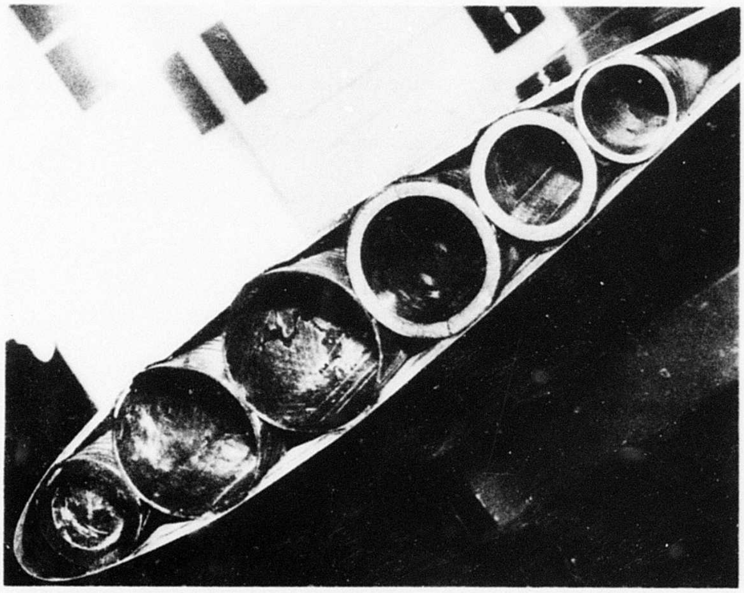

Figure 2. Finished end view of the HLH blade - cross section.

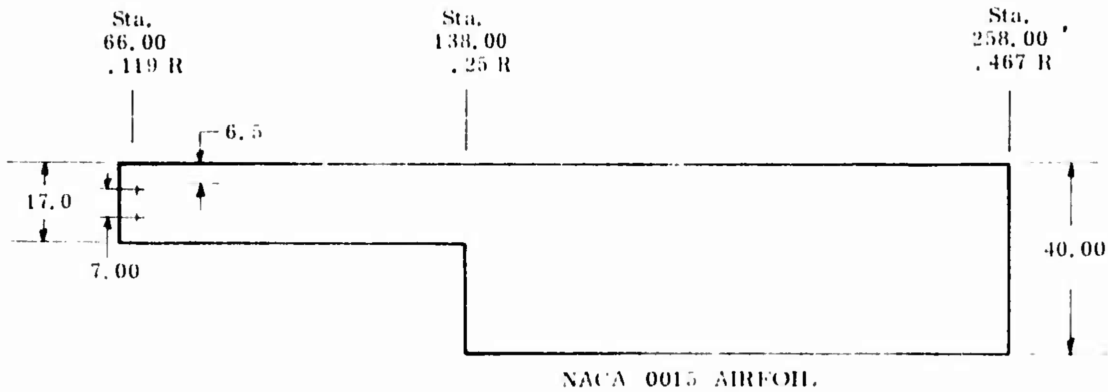

Figure 3. Blade section - external configuration.

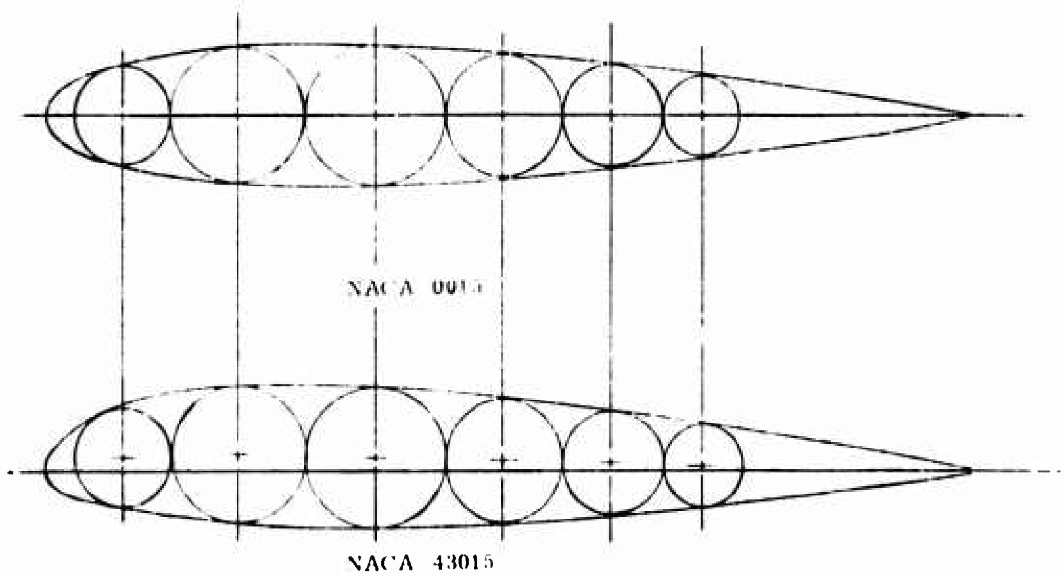

Figure 4. NACA 0015 and NACA 43015 airfoil configurations.

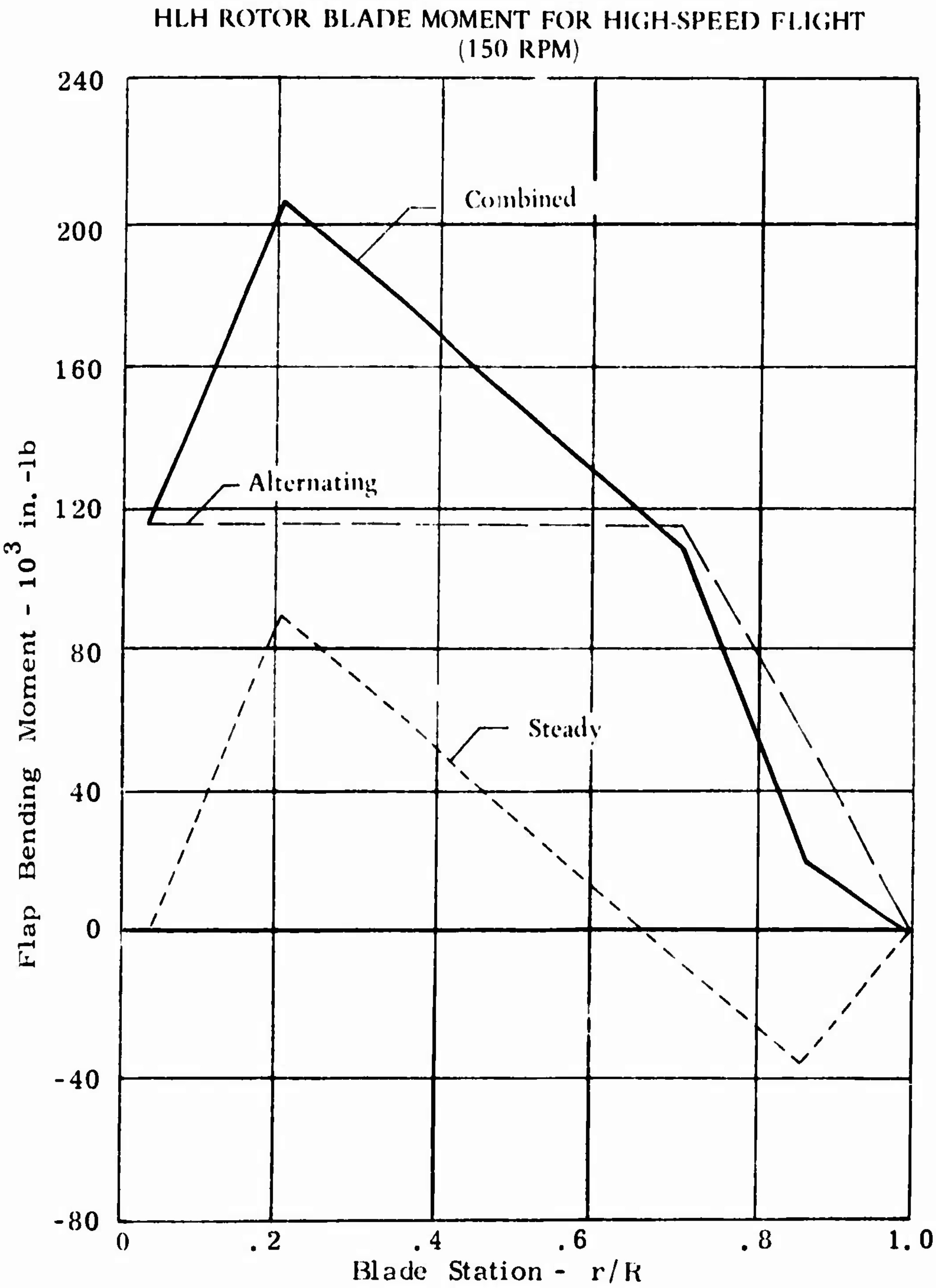

Figure 5. Flap bending moment versus blade station.

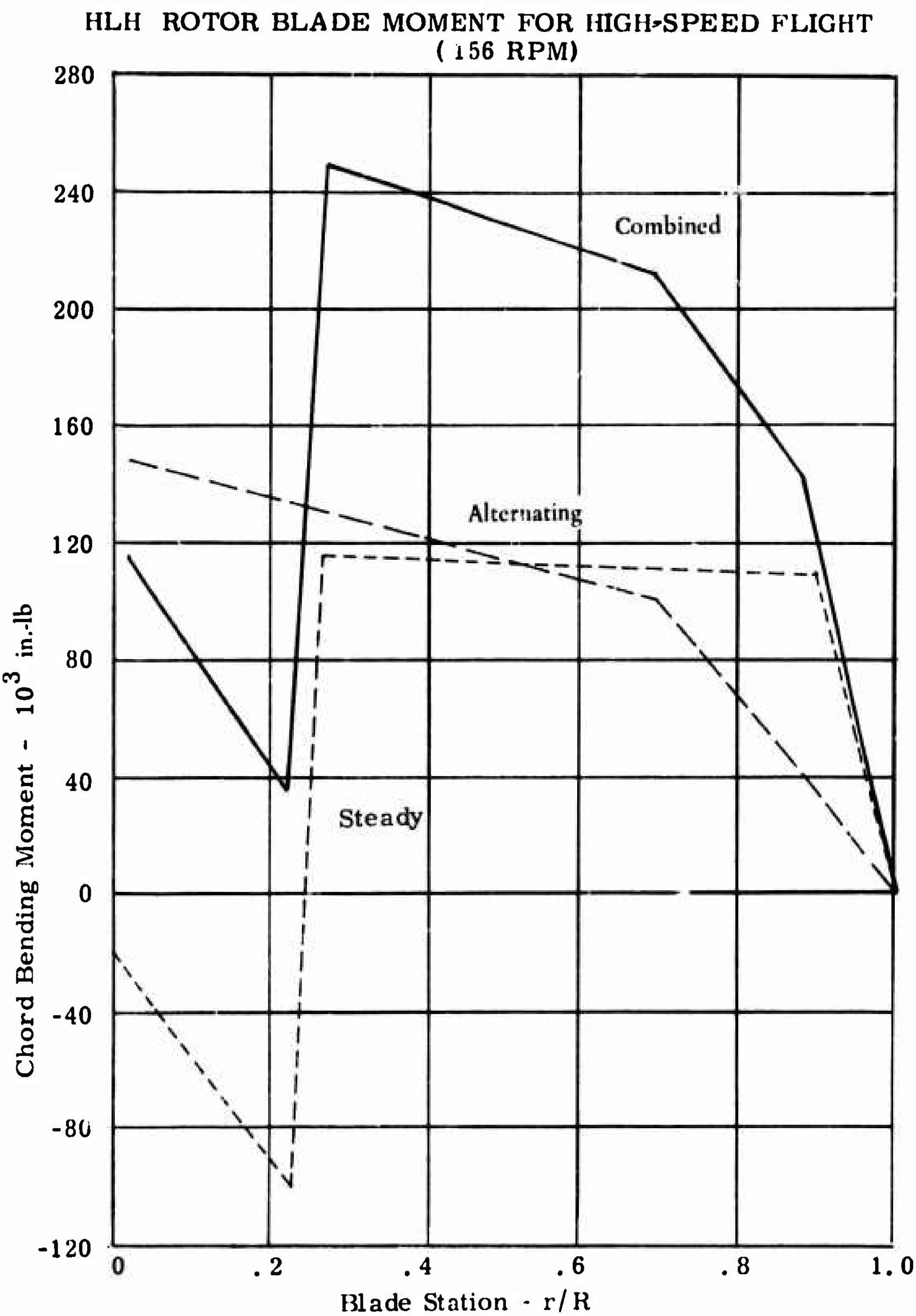

Figure 6. Chord bending moment versus blade station.

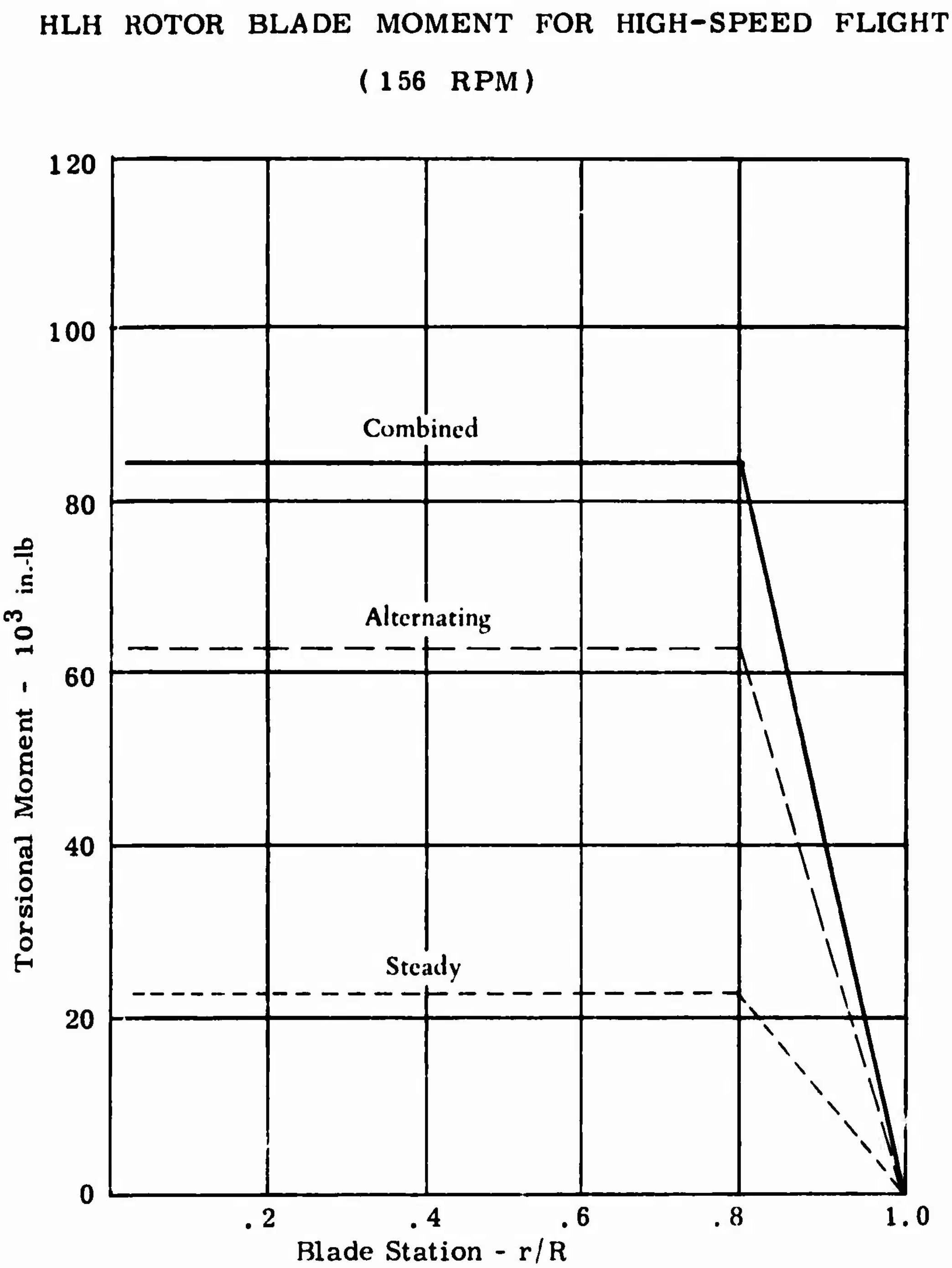

Figure 7. Torsional moment versus blade station.

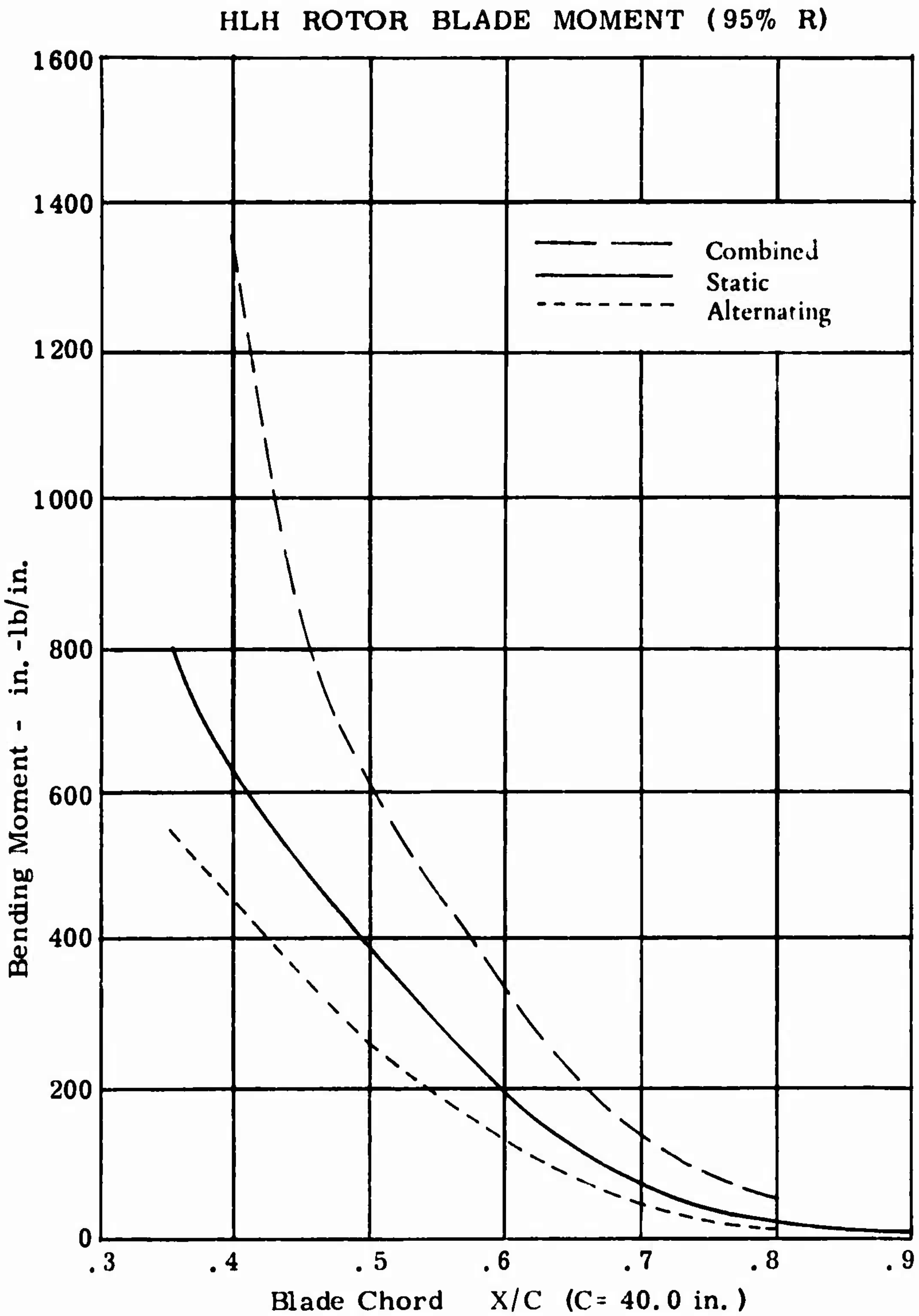

Figure 8. Bending moment versus blade chord.

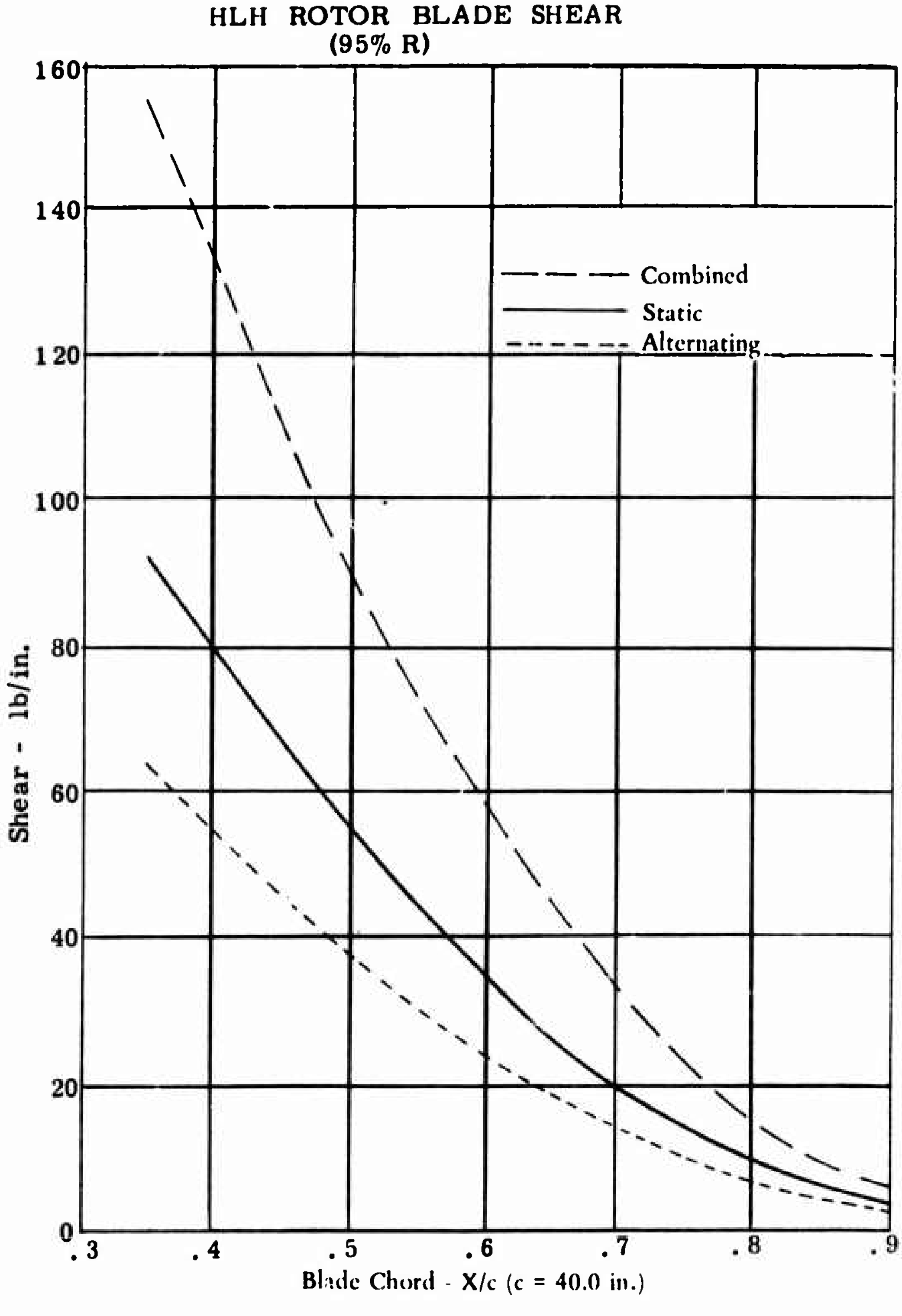

Figure 9. Shear versus blade chord.

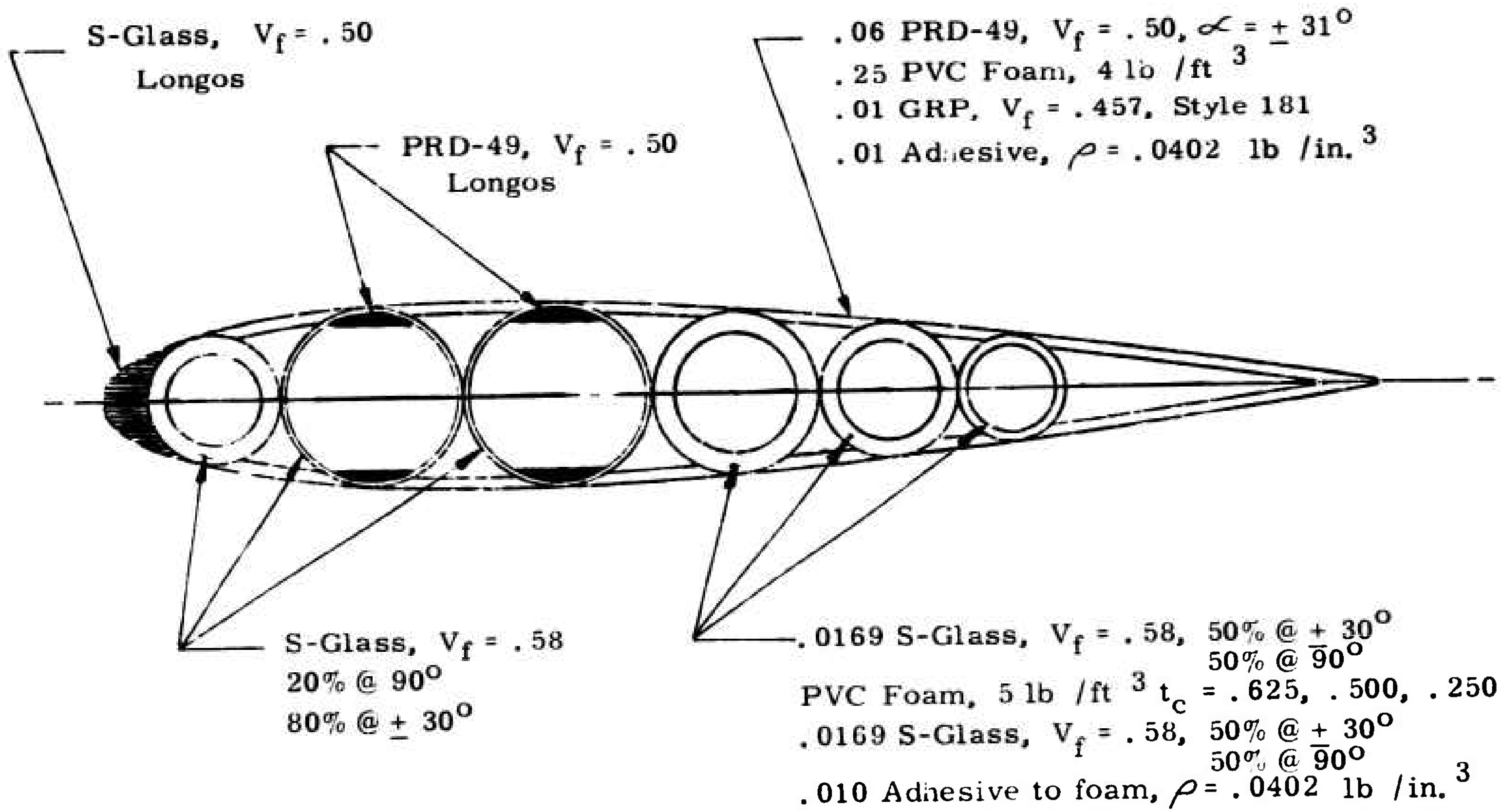

Figure 10. Blade design number 1.

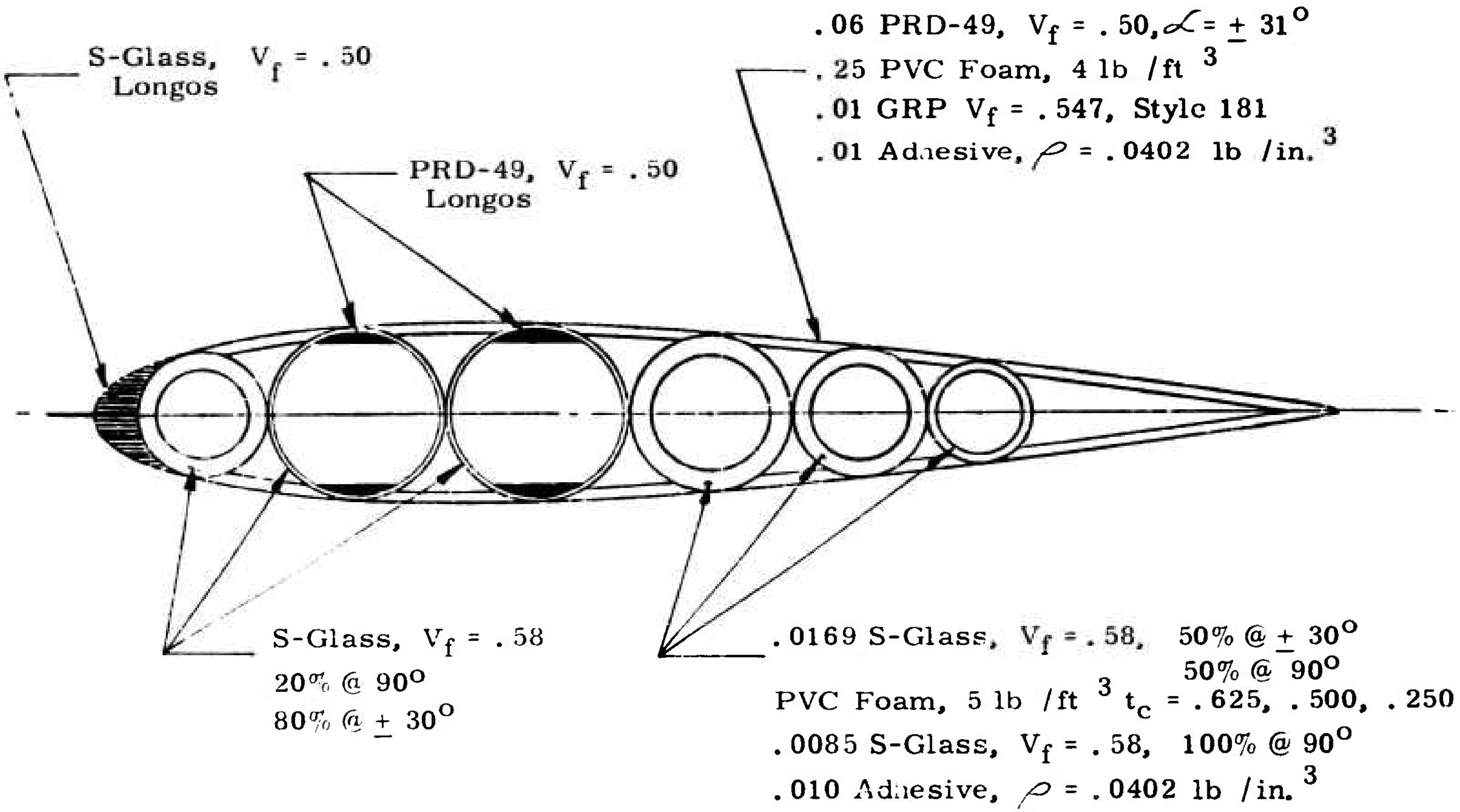

Figure 11. Blade design number 2.

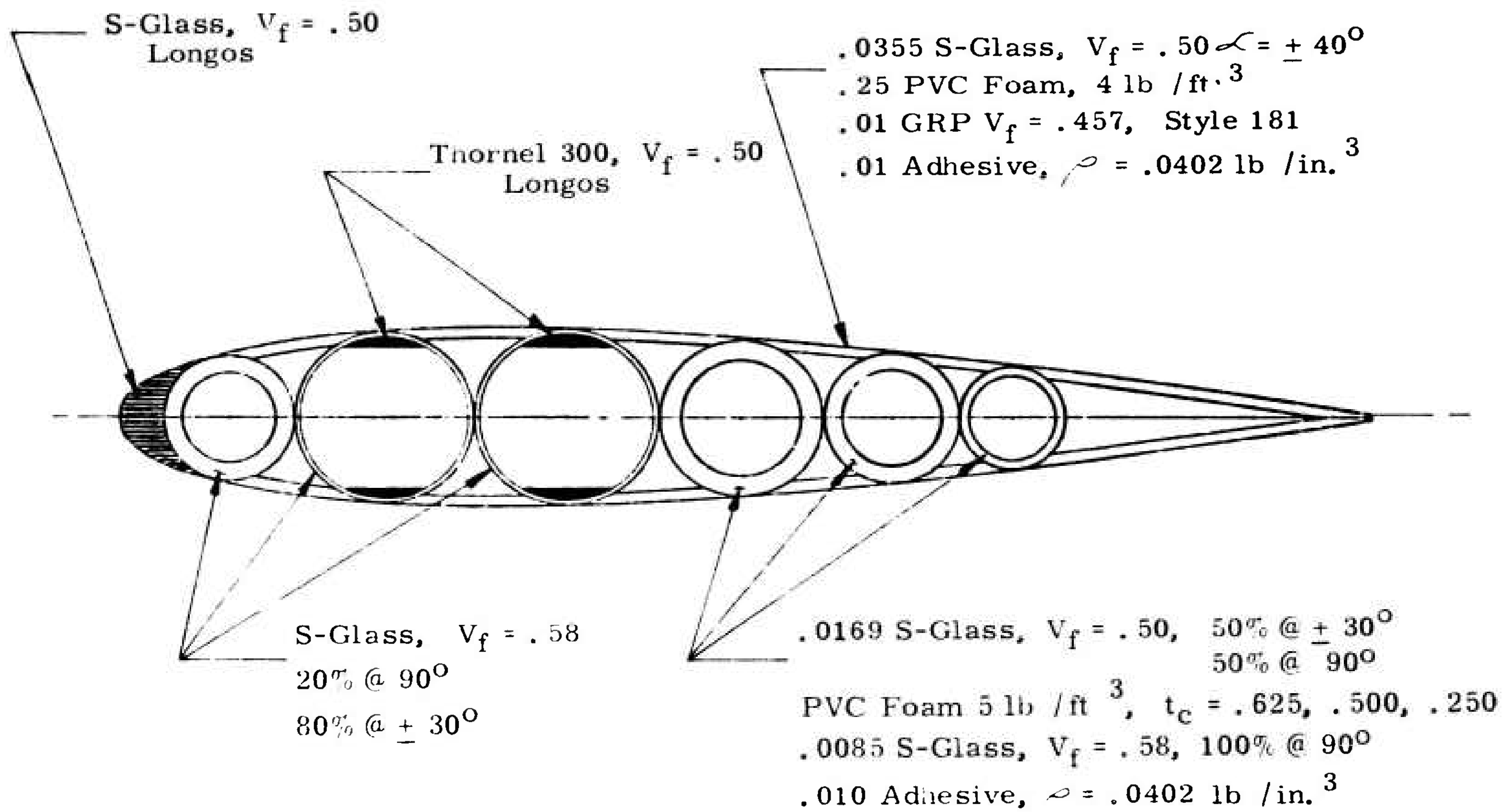

Figure 12. Blade design number 3.

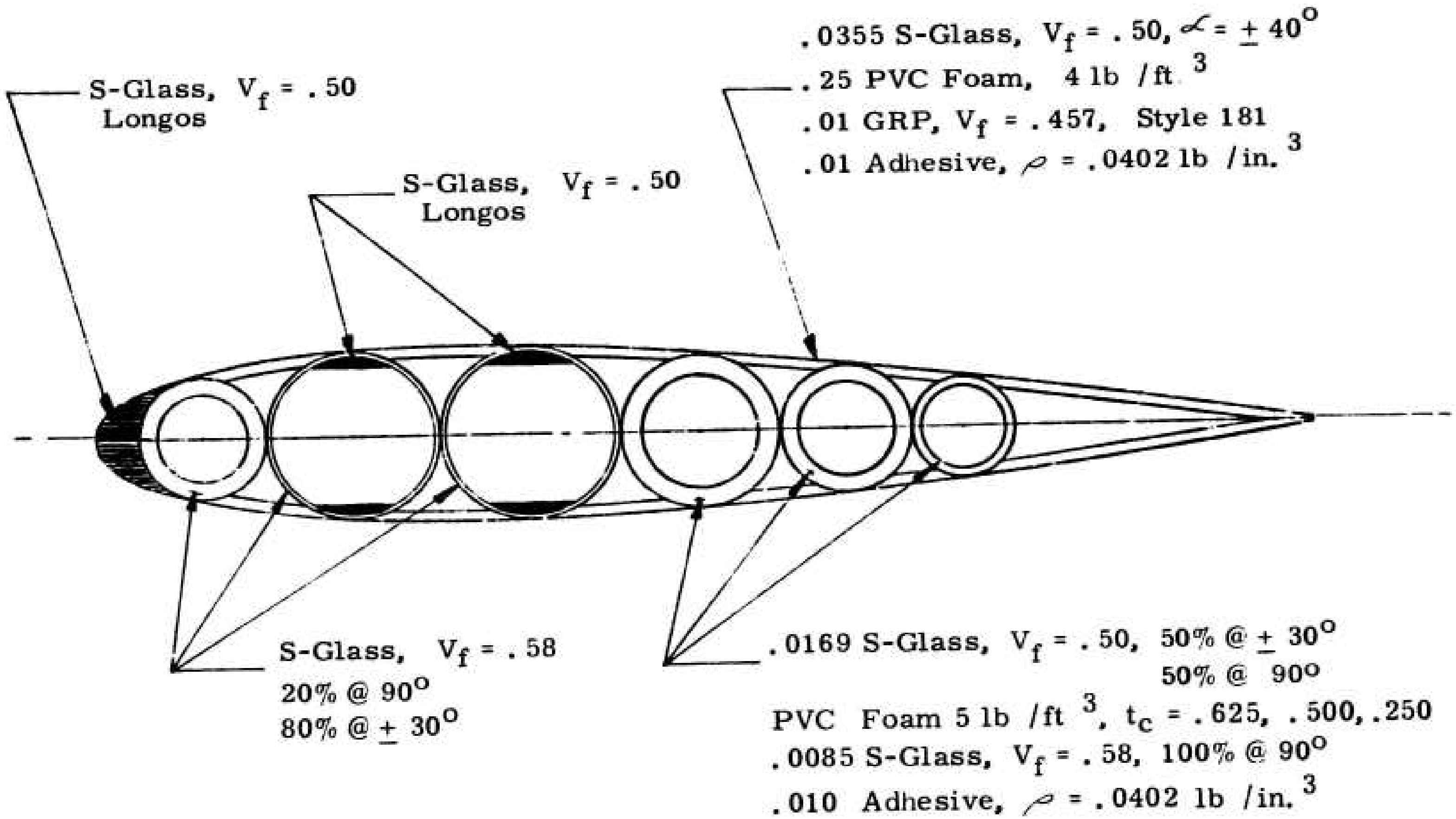

Figure 13. Blade design number 4.

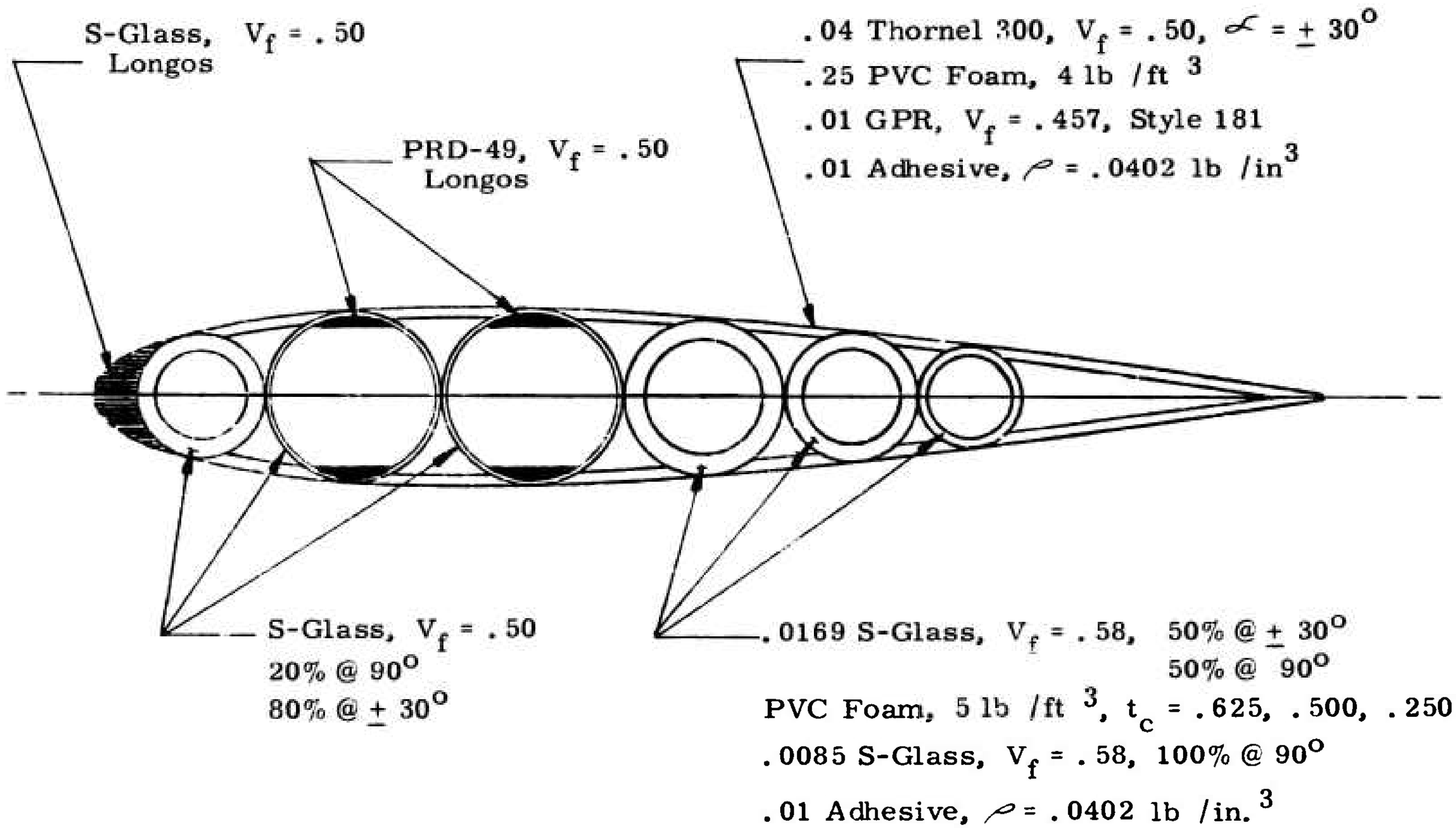

Figure 14. Blade design number 5.

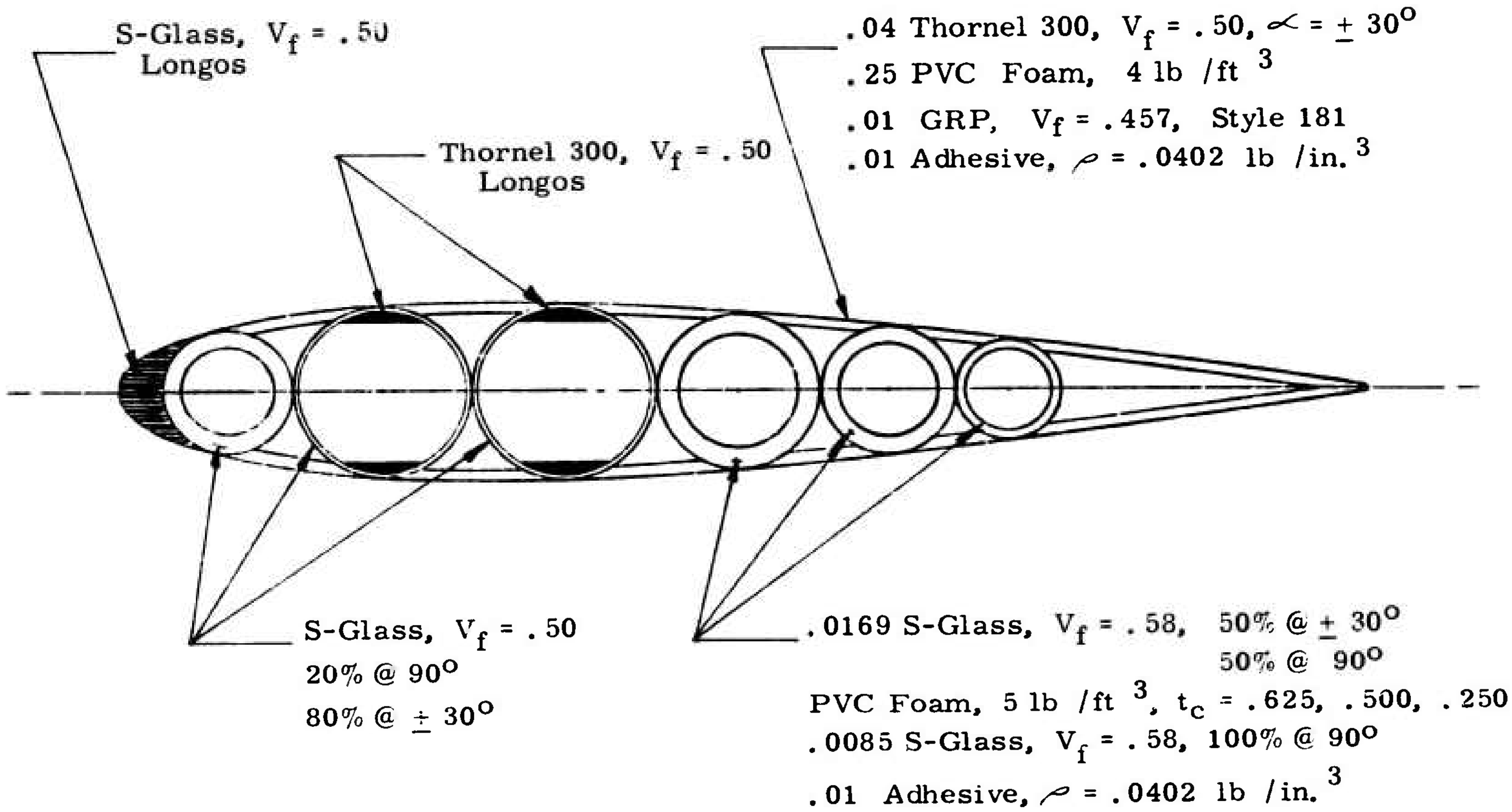

Figure 15. Blade designs numbers 6 and 6A.

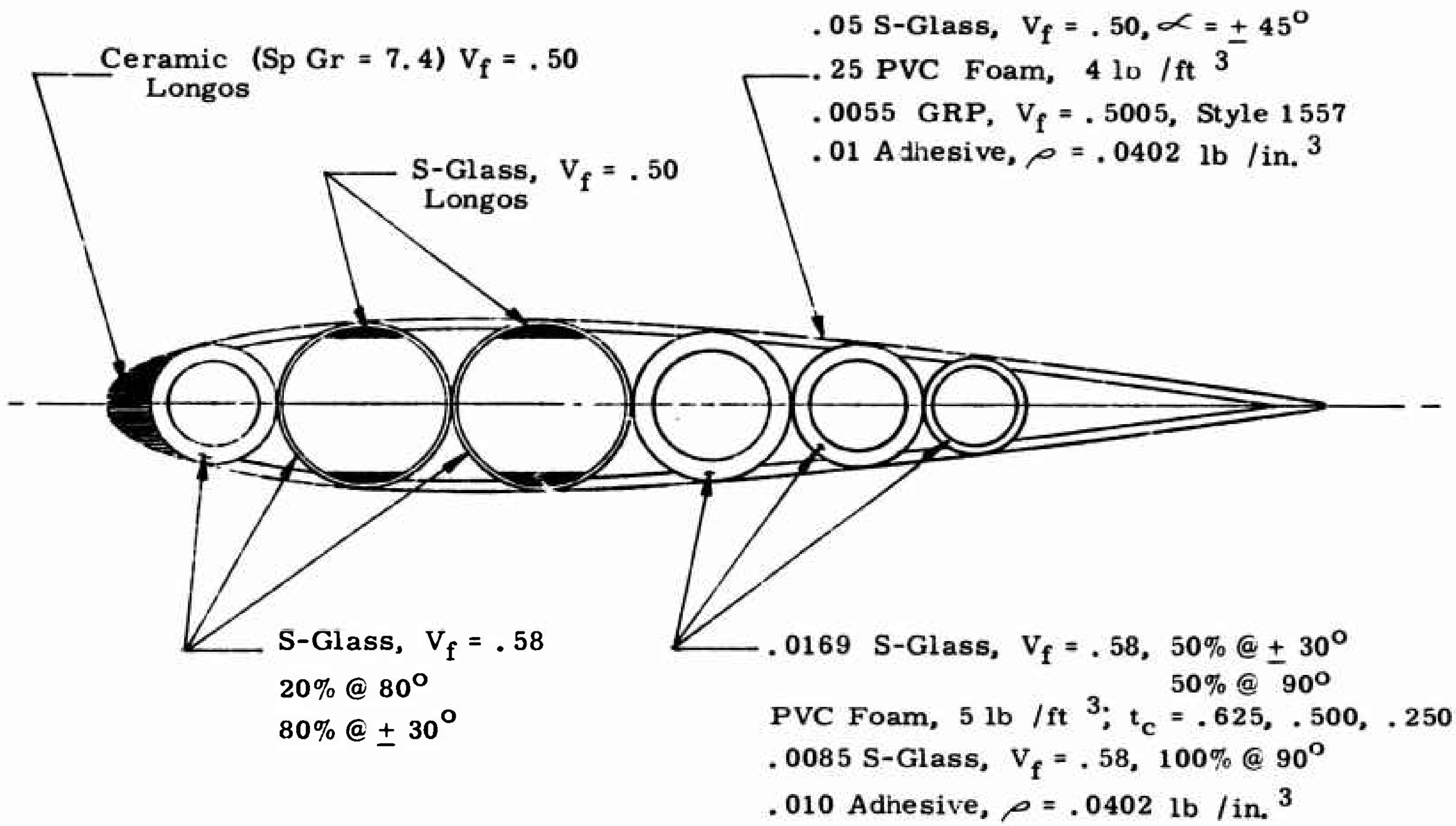

Figure 16. Blade design number 7.

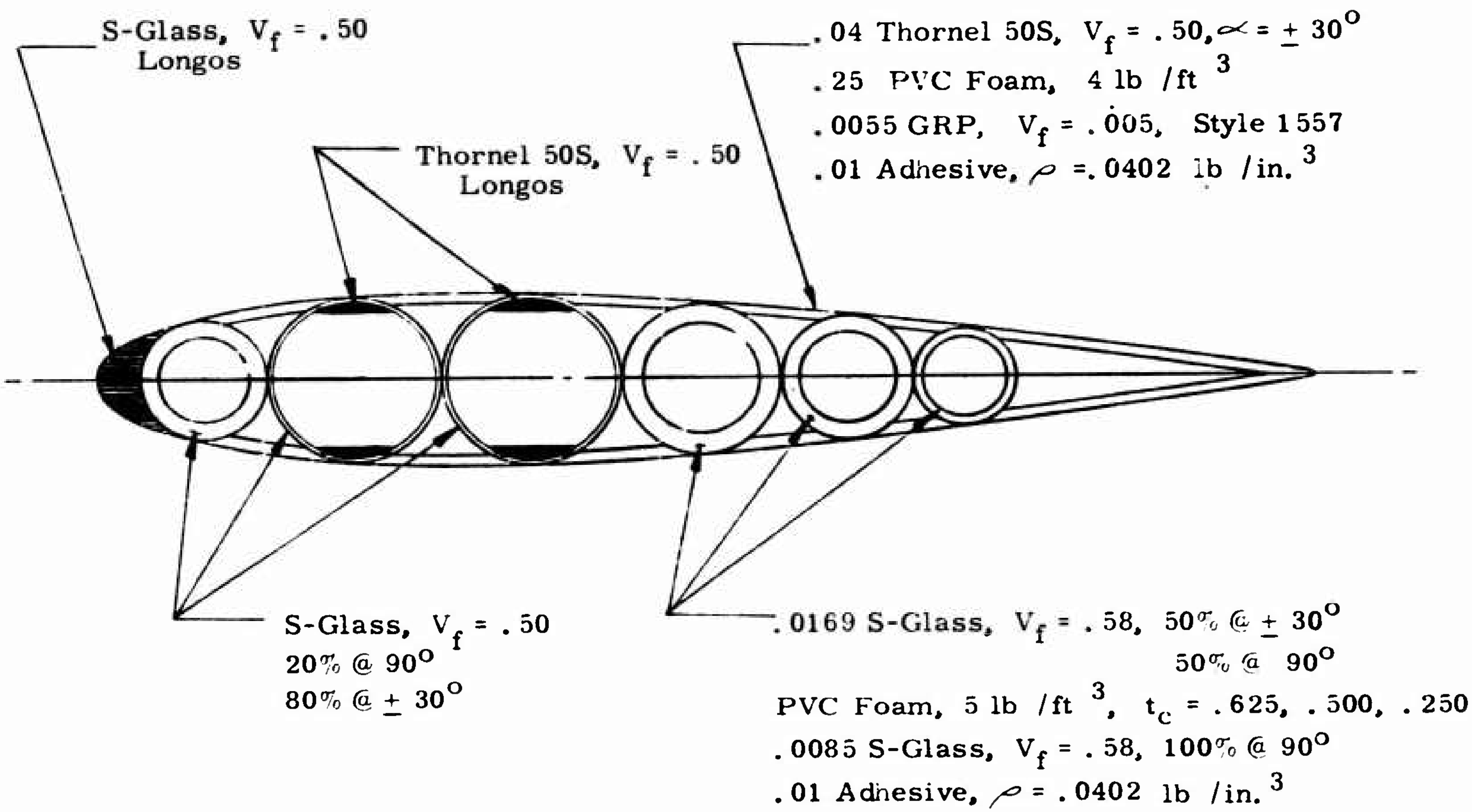

Figure 17. Blade design number 8.

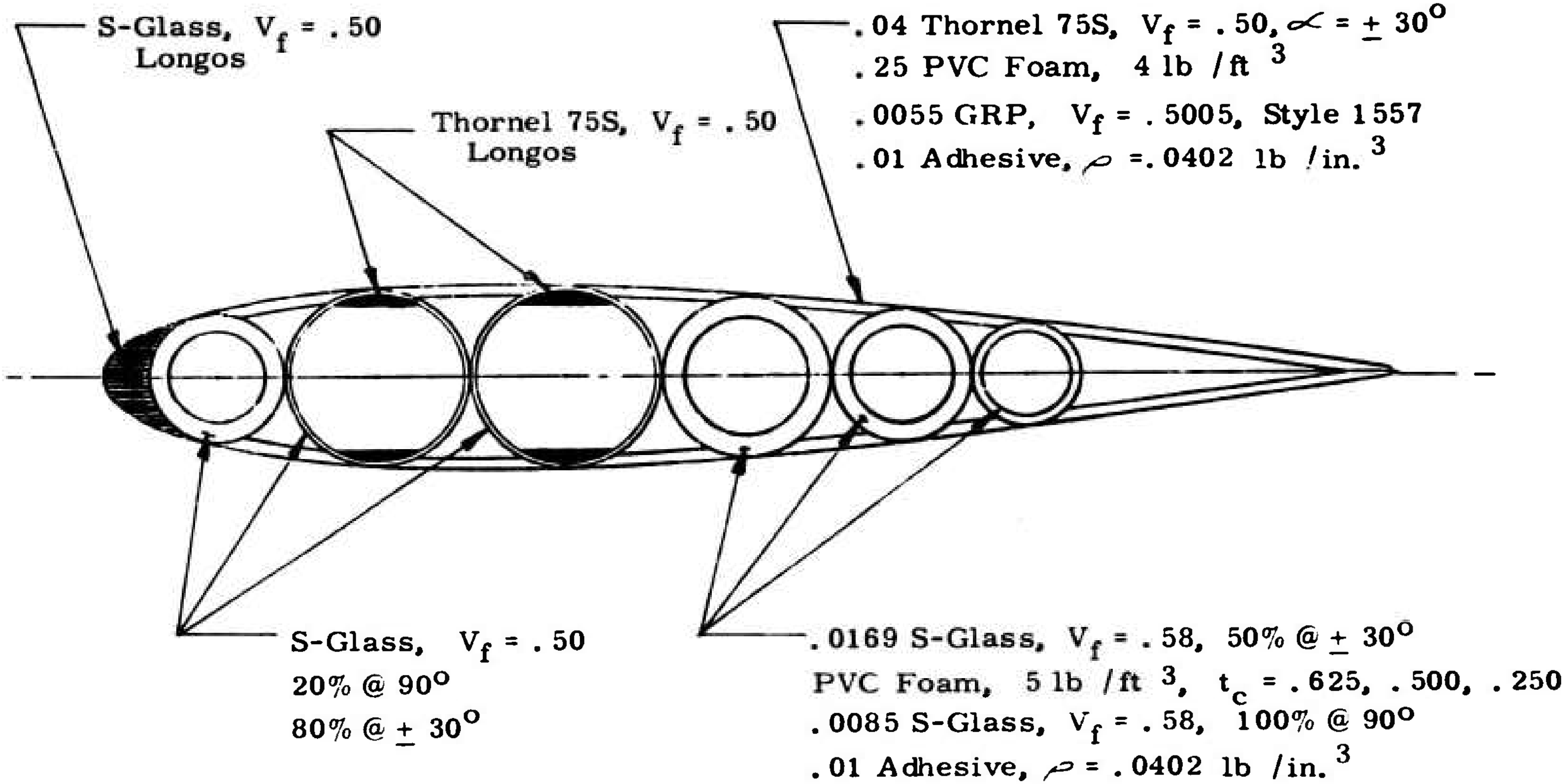

Figure 18. Blade design number 9.

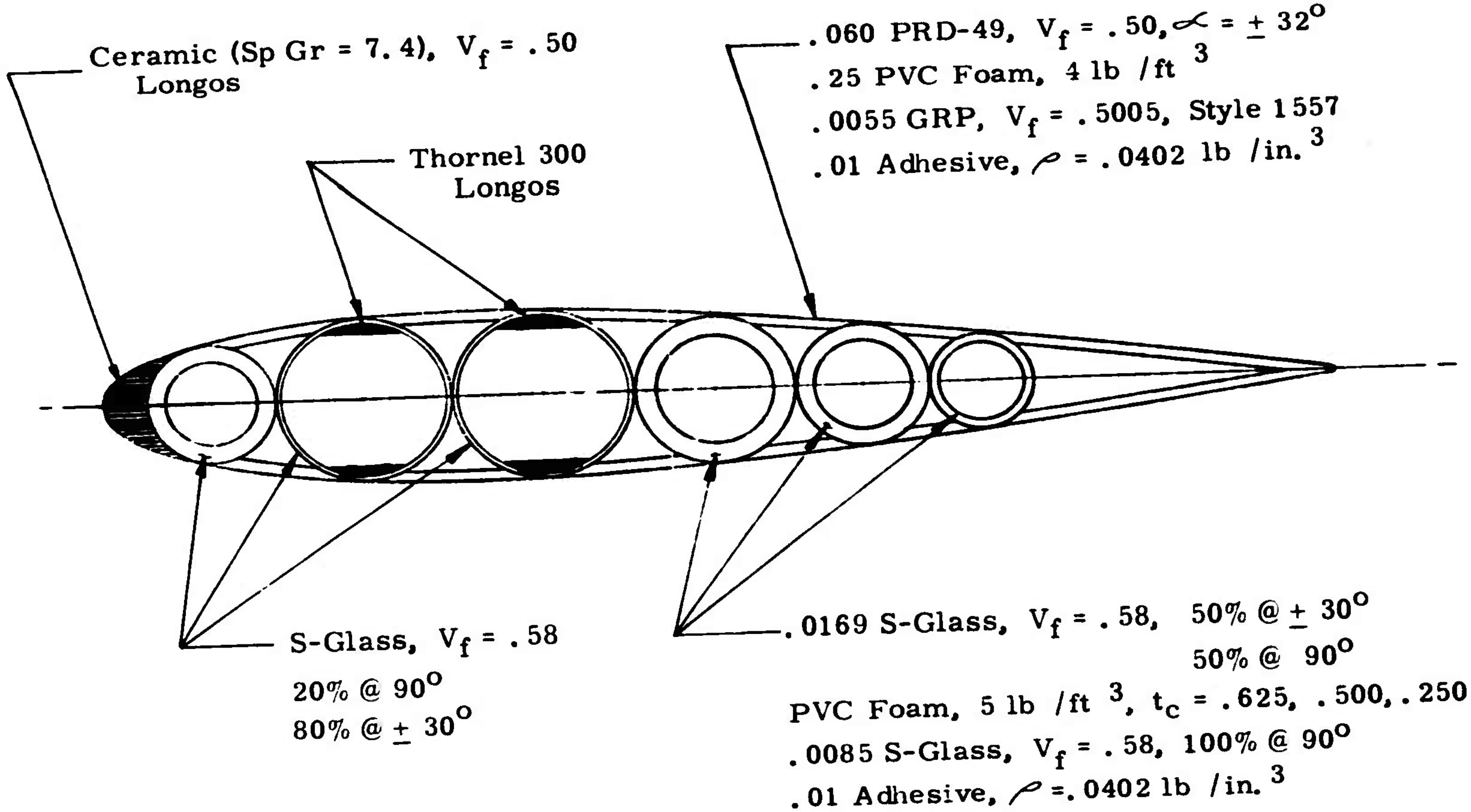

Figure 19. Blade design number 10.

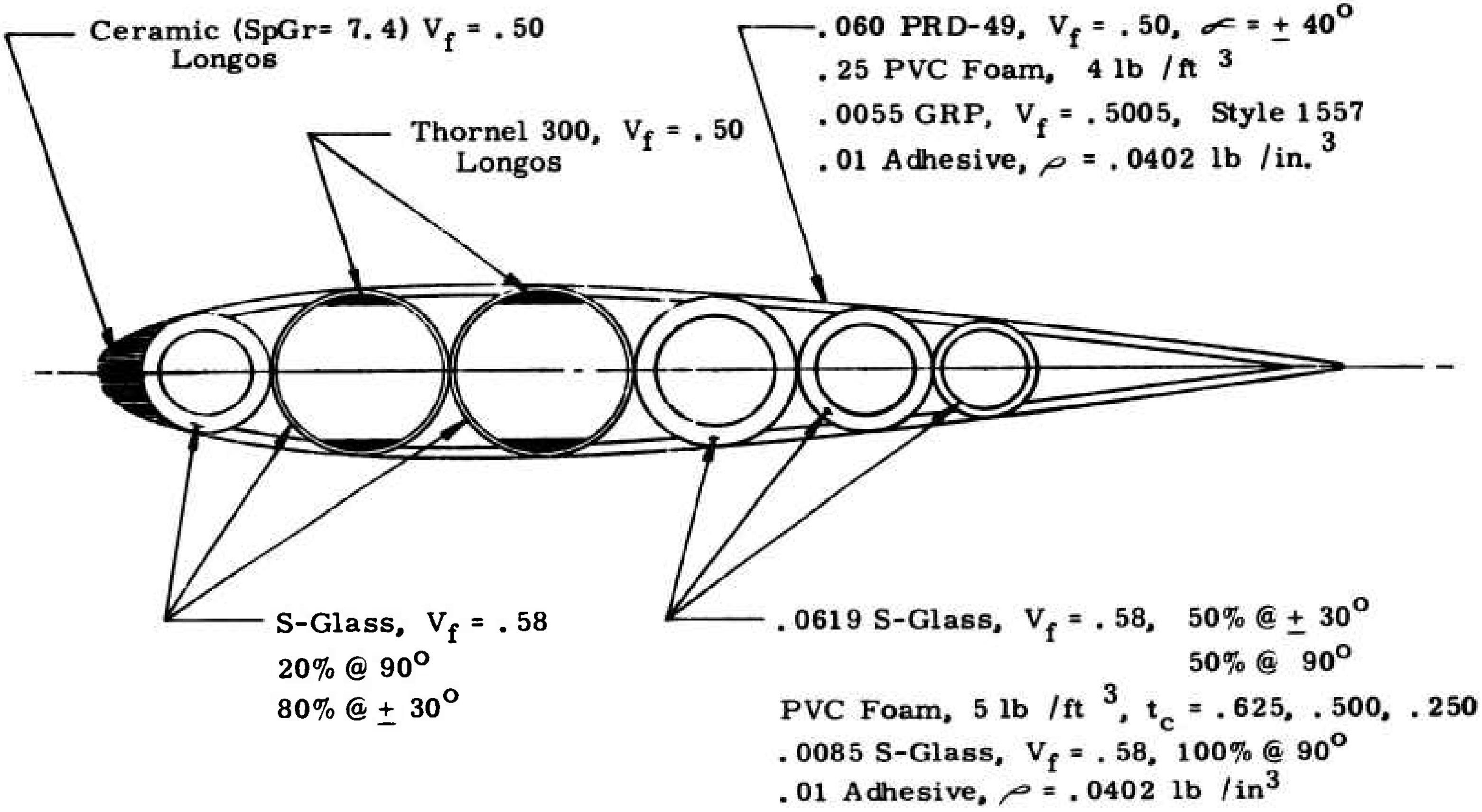

Figure 20. Blade design number 11.

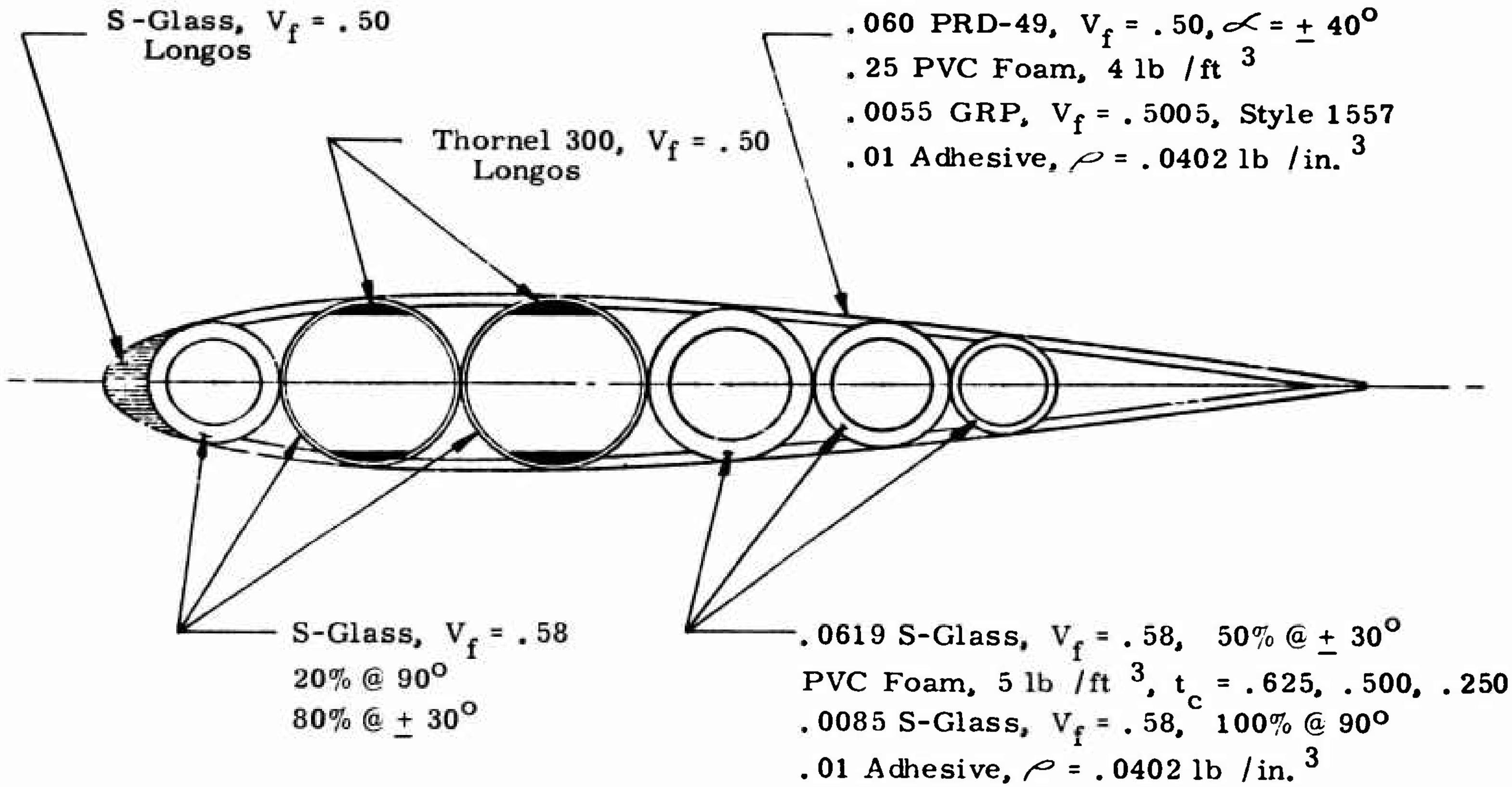

Figure 21. Blade designs numbers 12 and 12A.

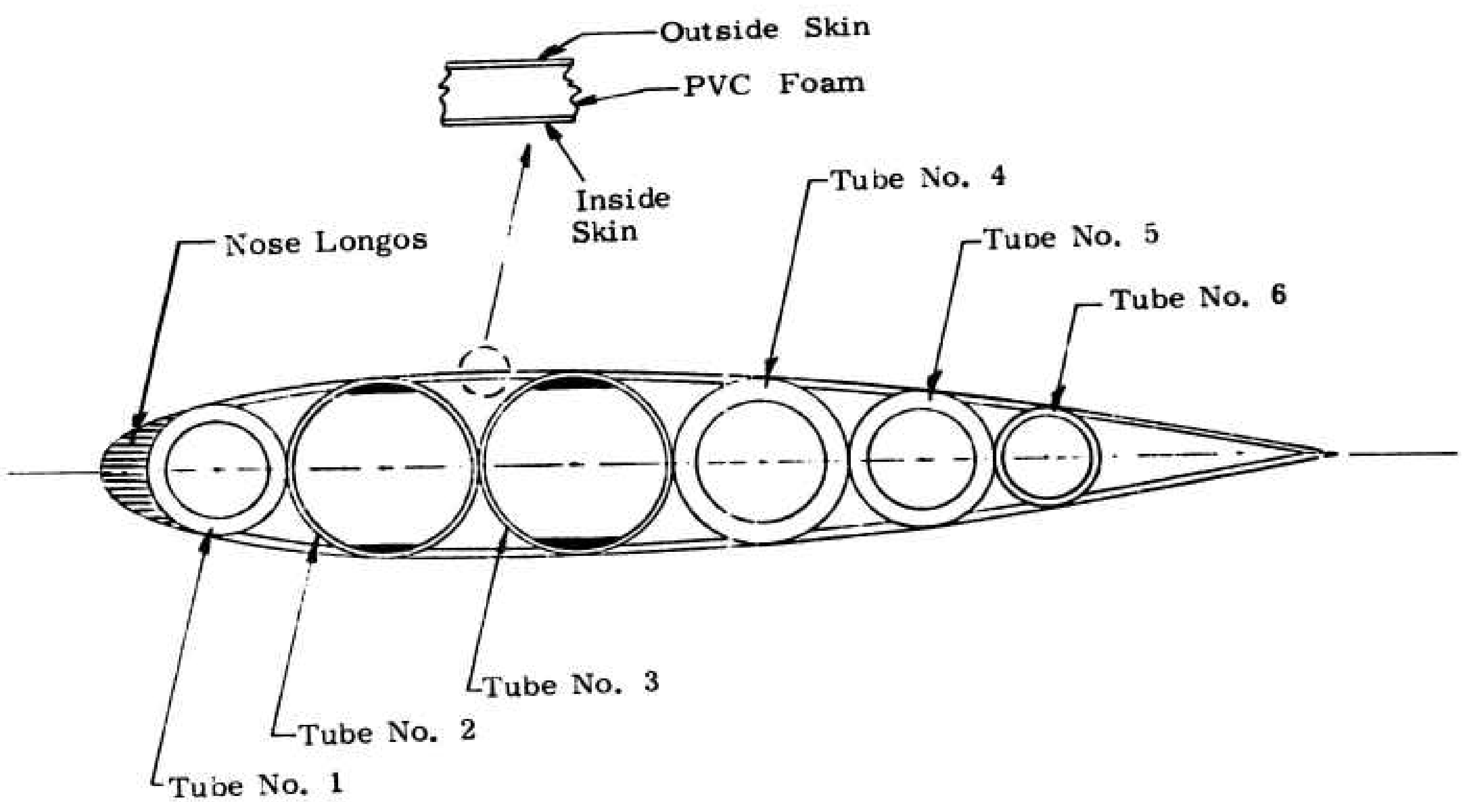

Figure 22. Tubular composite rotor blade cross section.

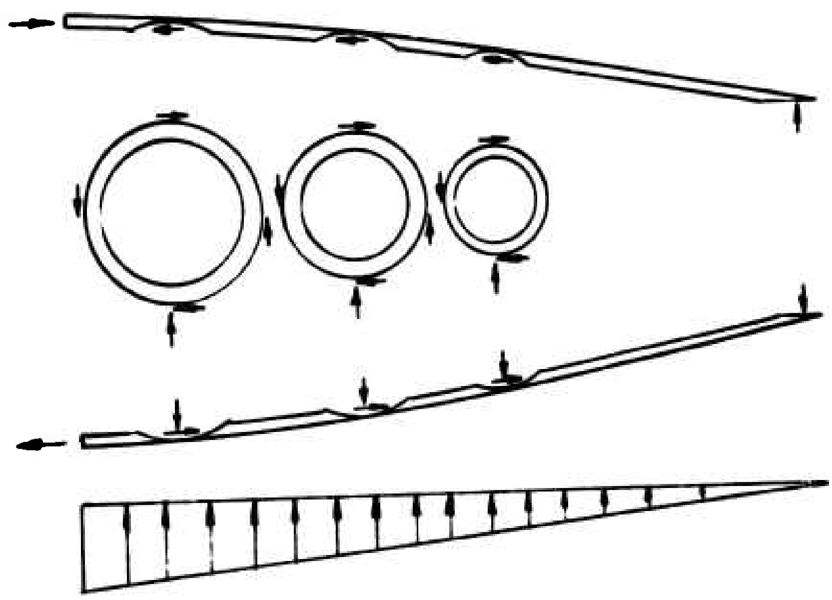

Figure 23. Aft tubes and skin free-body diagram.

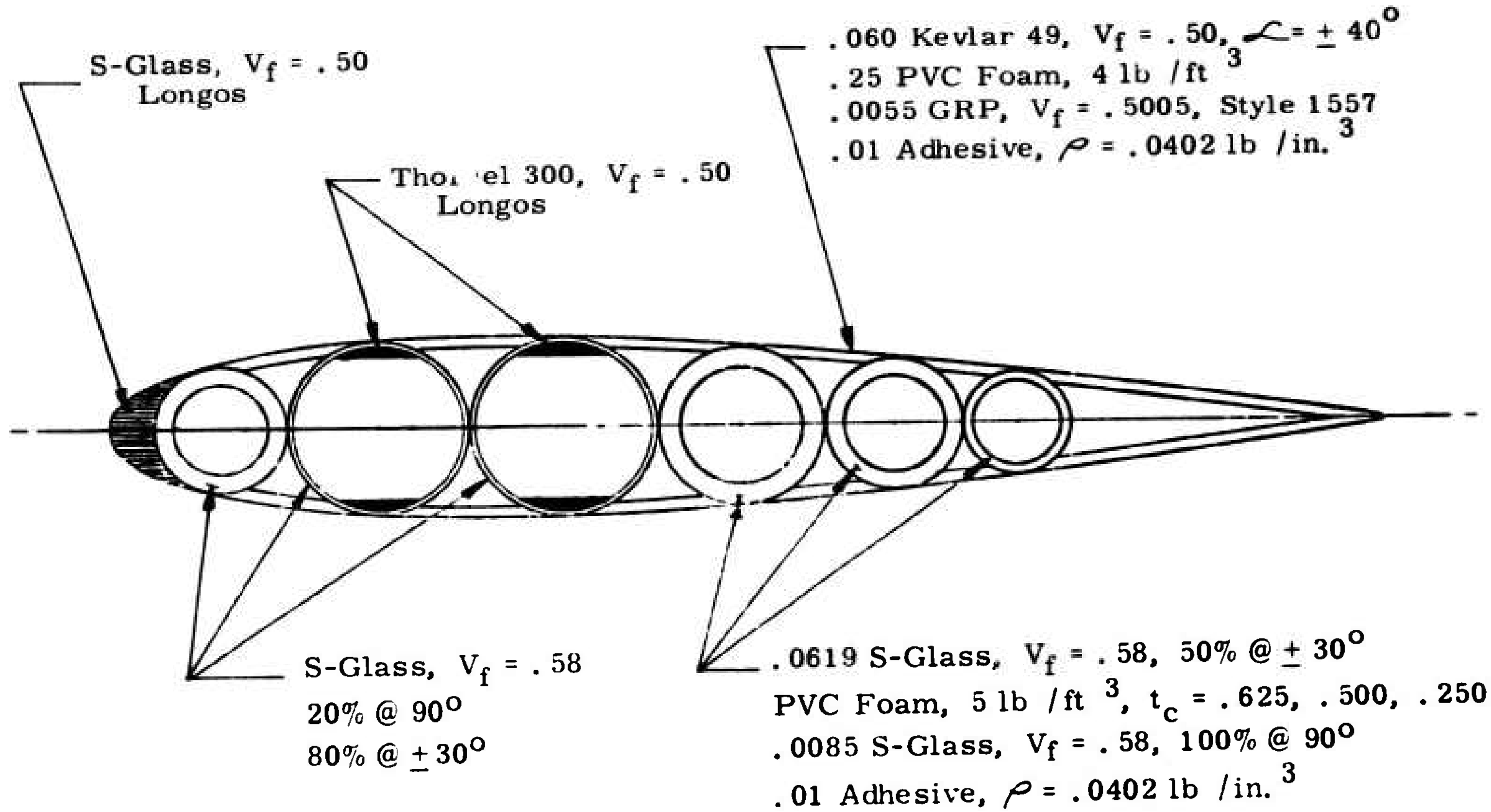

Figure 24. Tubular composite rotor blade cross section, showing materials used.

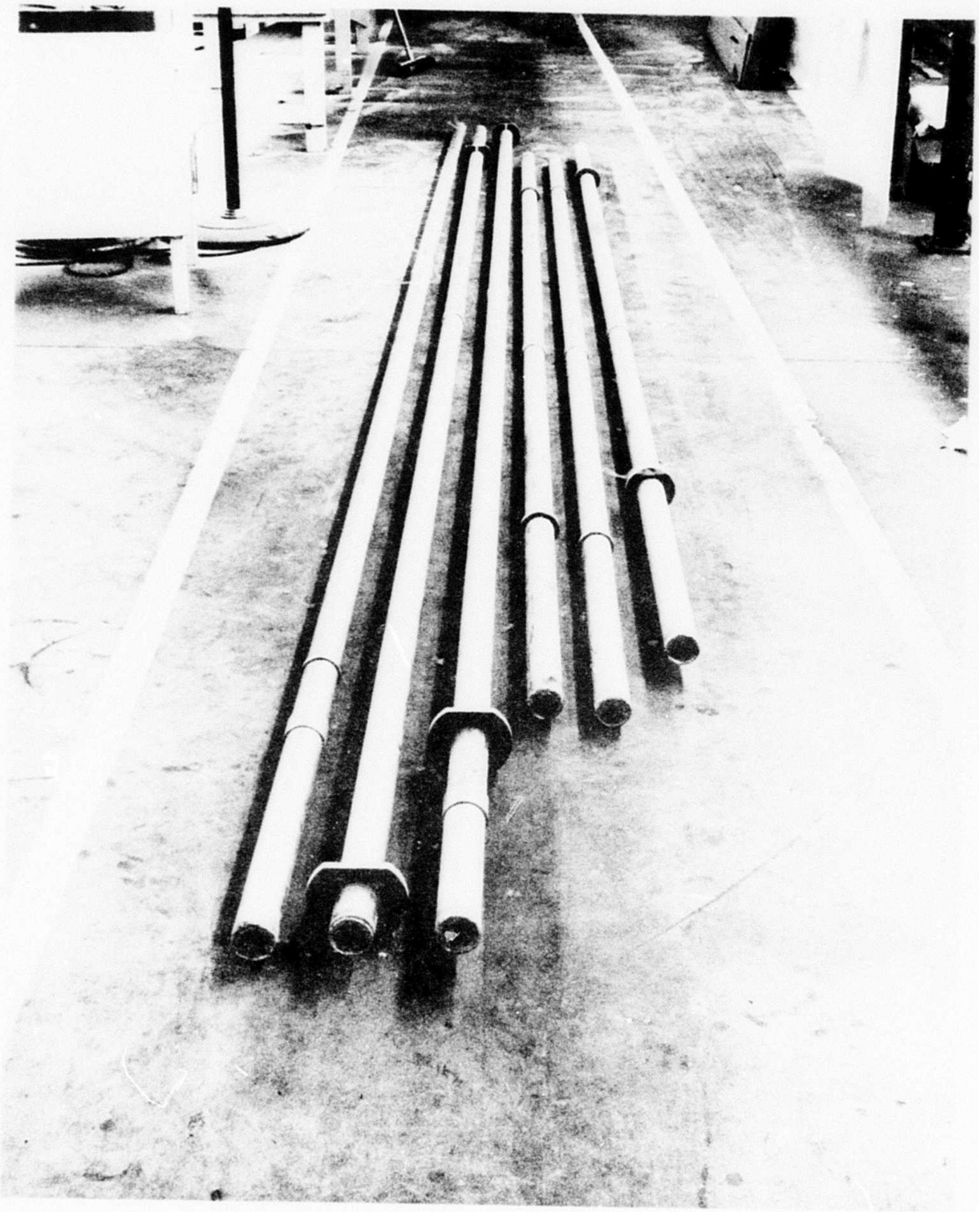

Figure 25. Tube winding hardware ready to have plastic bags attached.

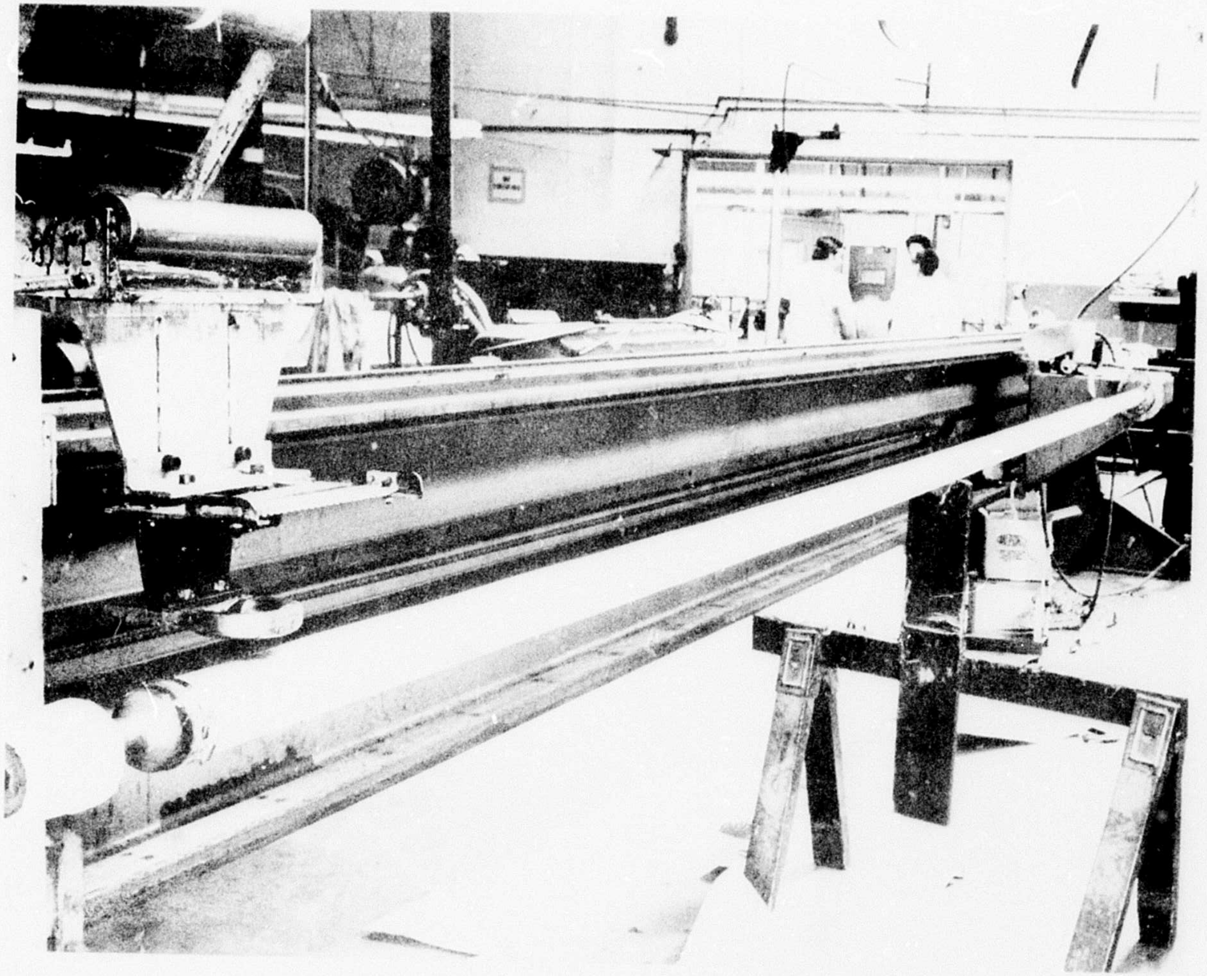

Figure 26. Tube mandrel ready for winding.

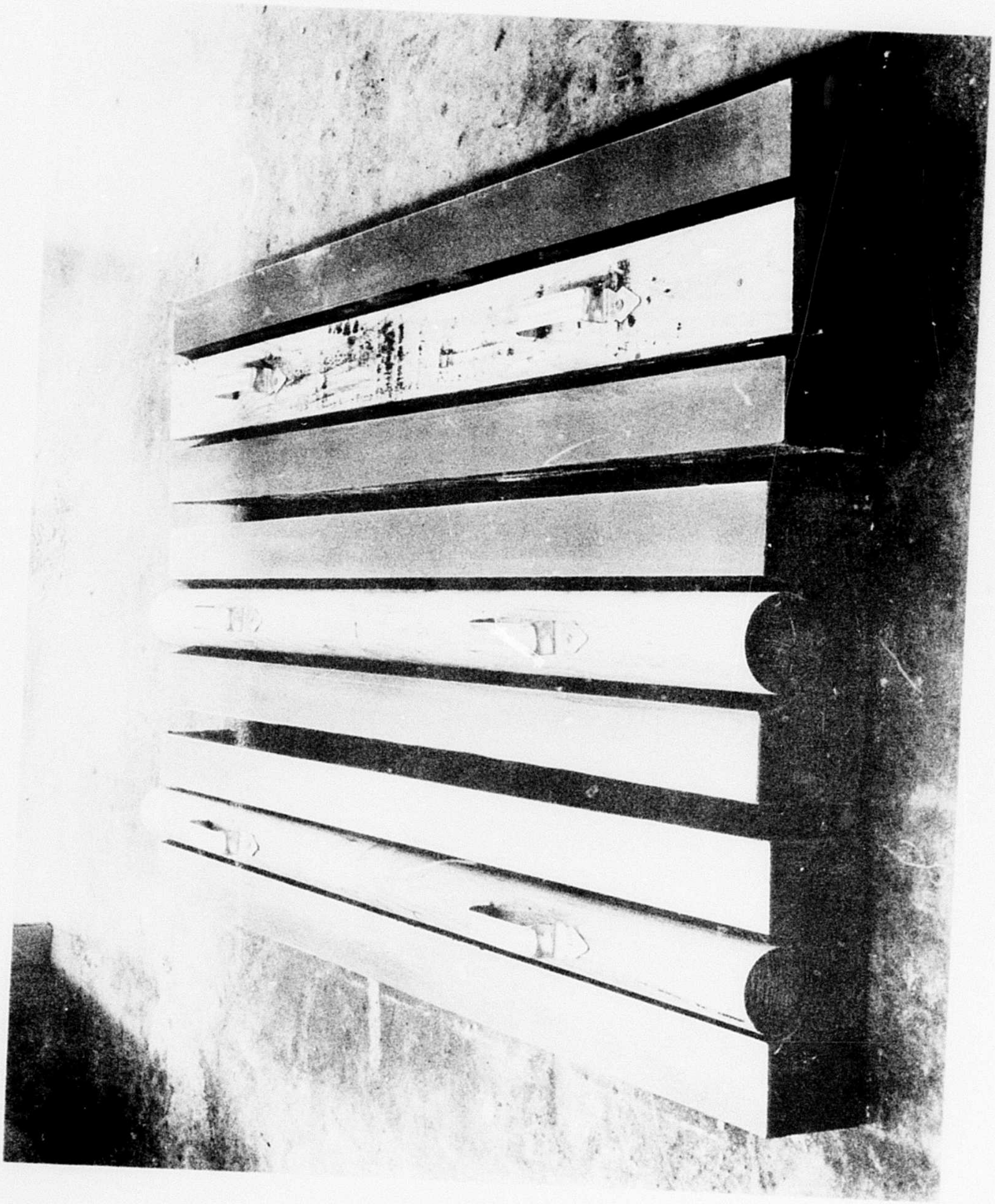

Figure 27. Tube foam-forming molds.

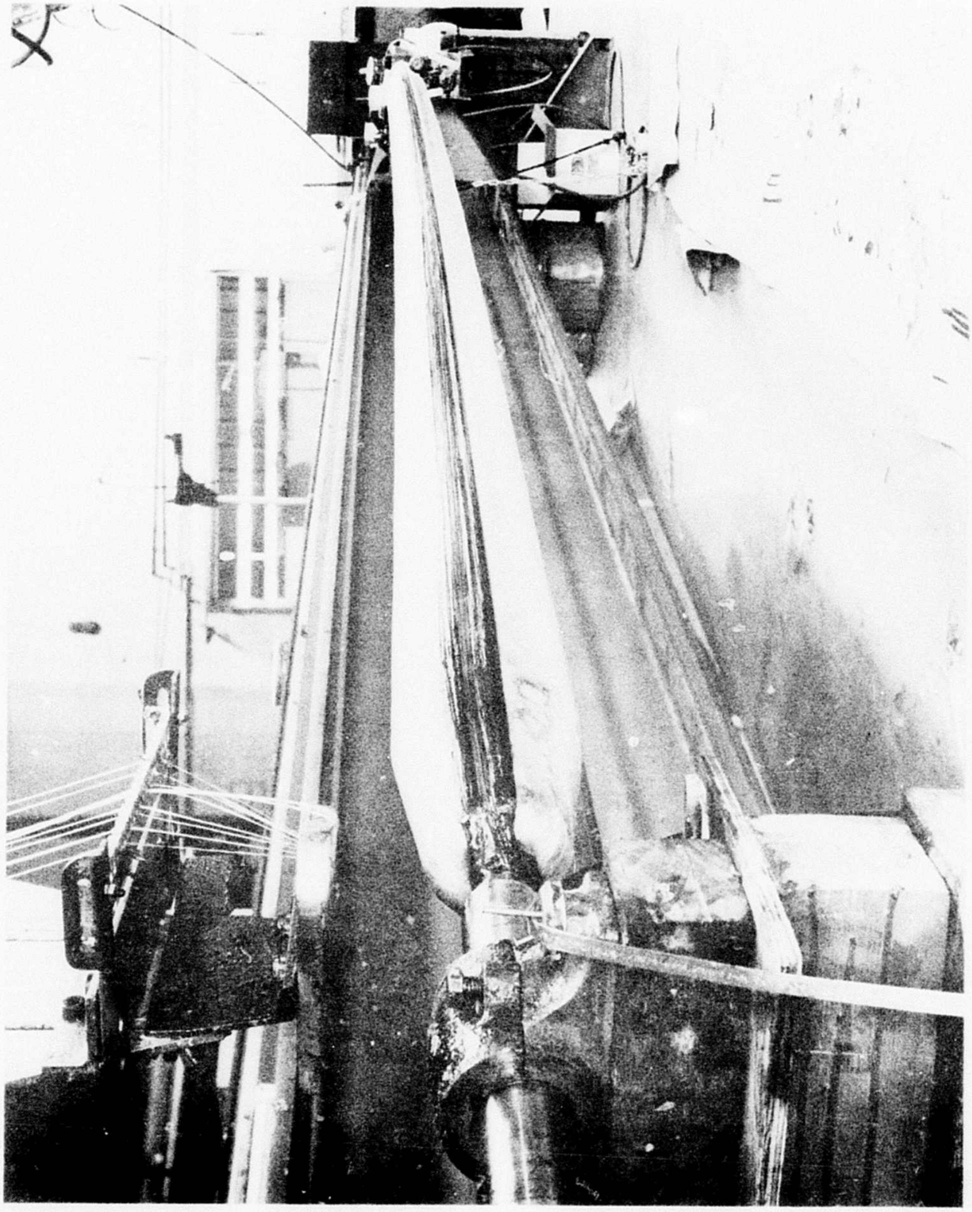

Figure 28. Tube winding, showing longo material.

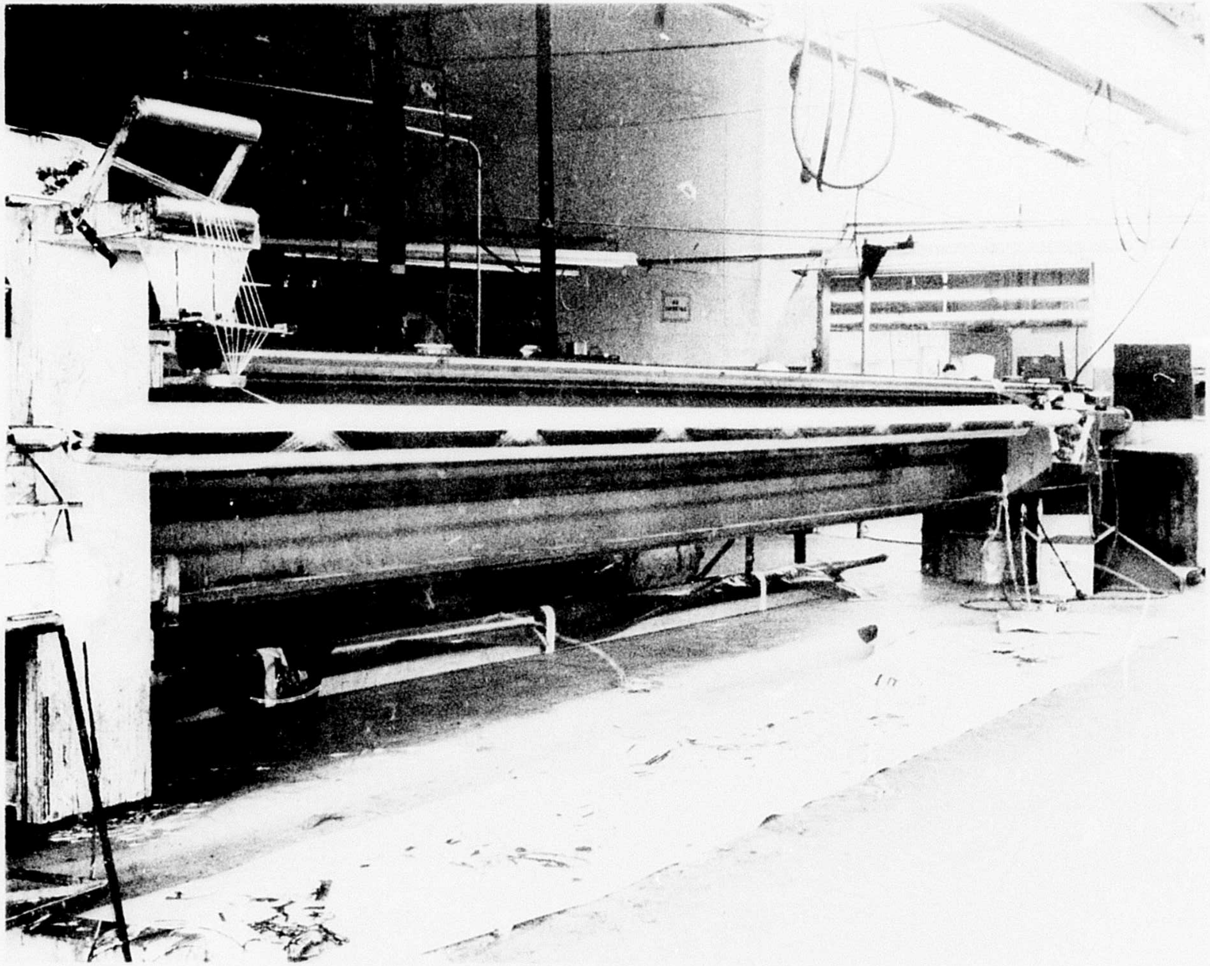

Figure 29. Tube winding, showing start of helical overwinding of the longo material.

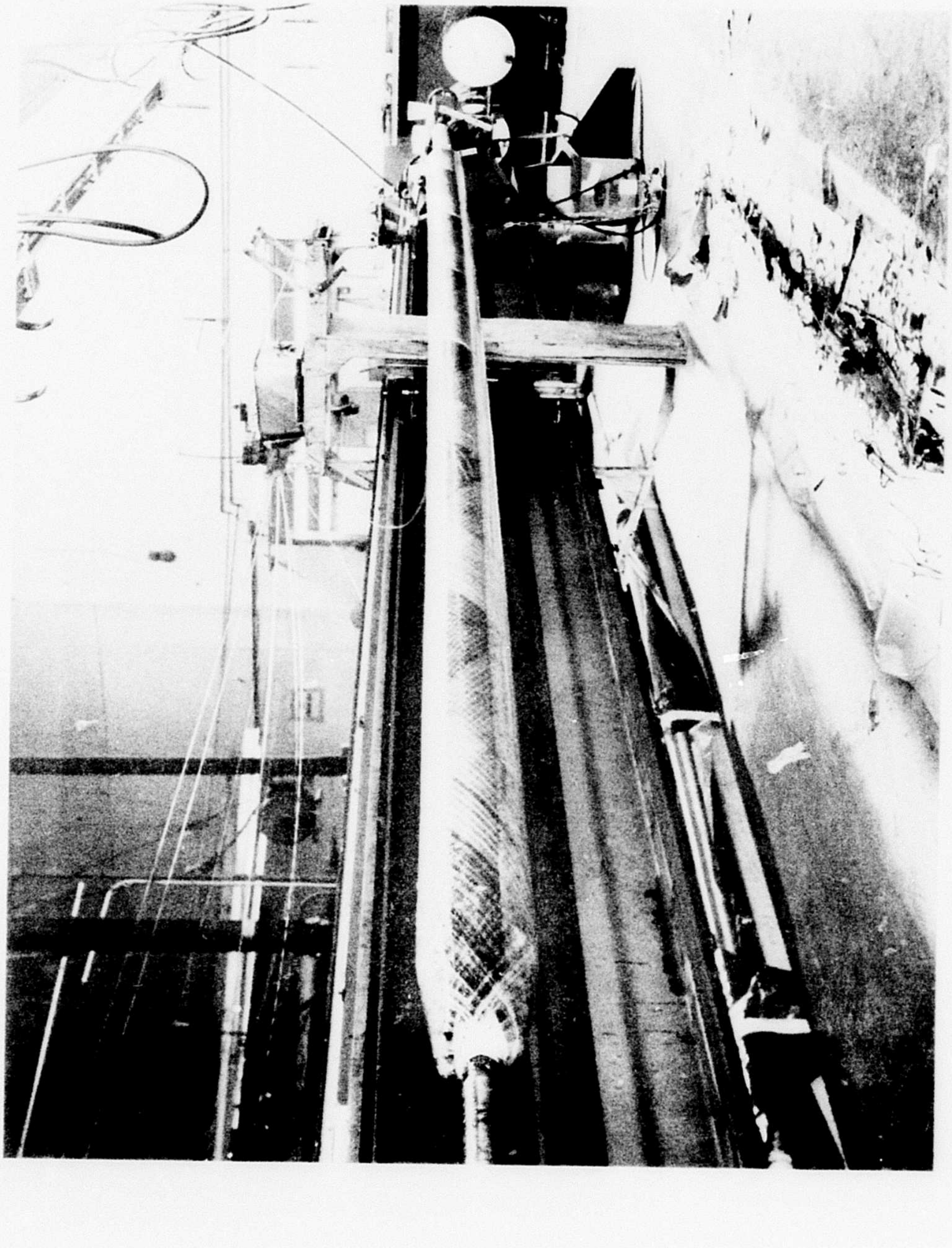

Figure 30. Tube winding near completion.

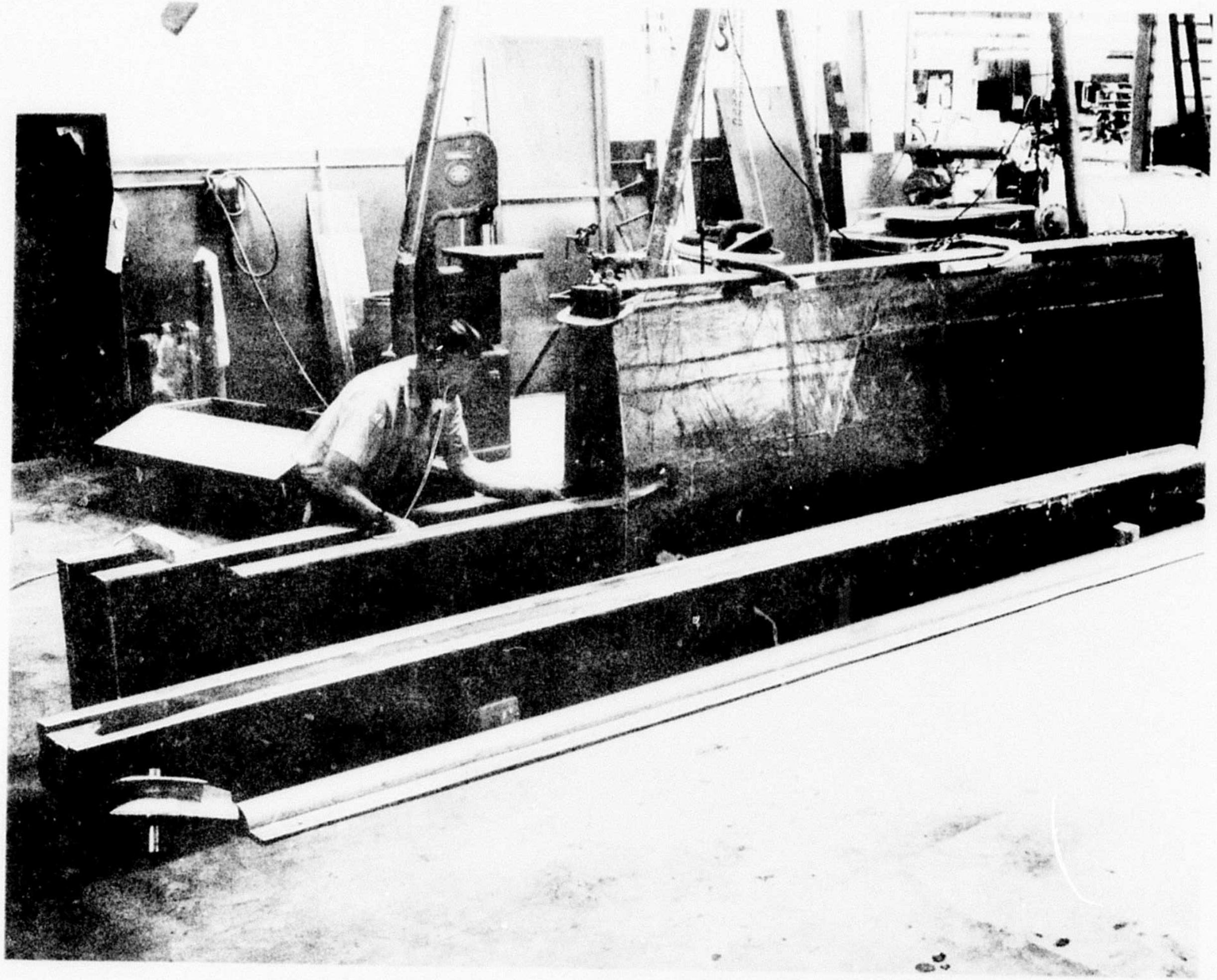

Figure 31. Skin and nose longo molds.

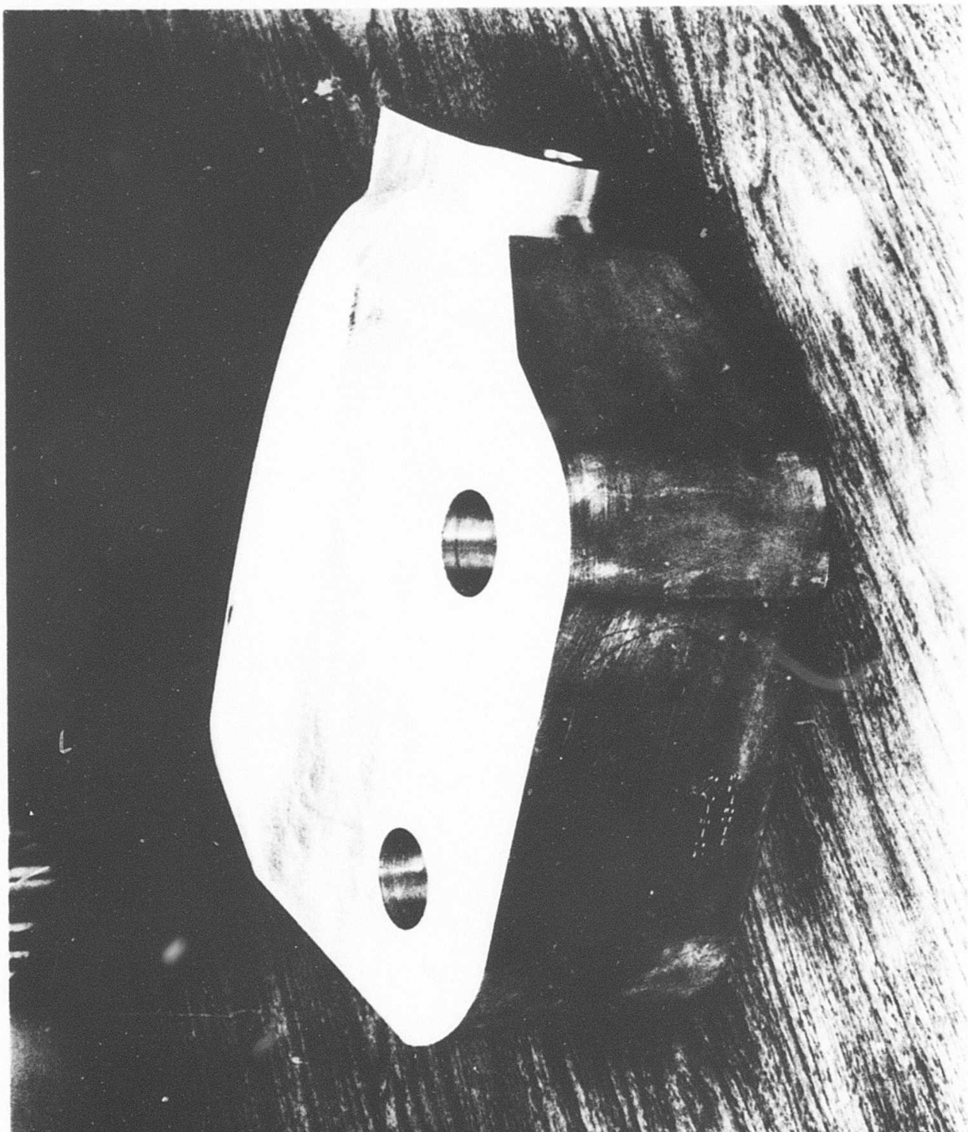

Figure 32. Root end fitting.

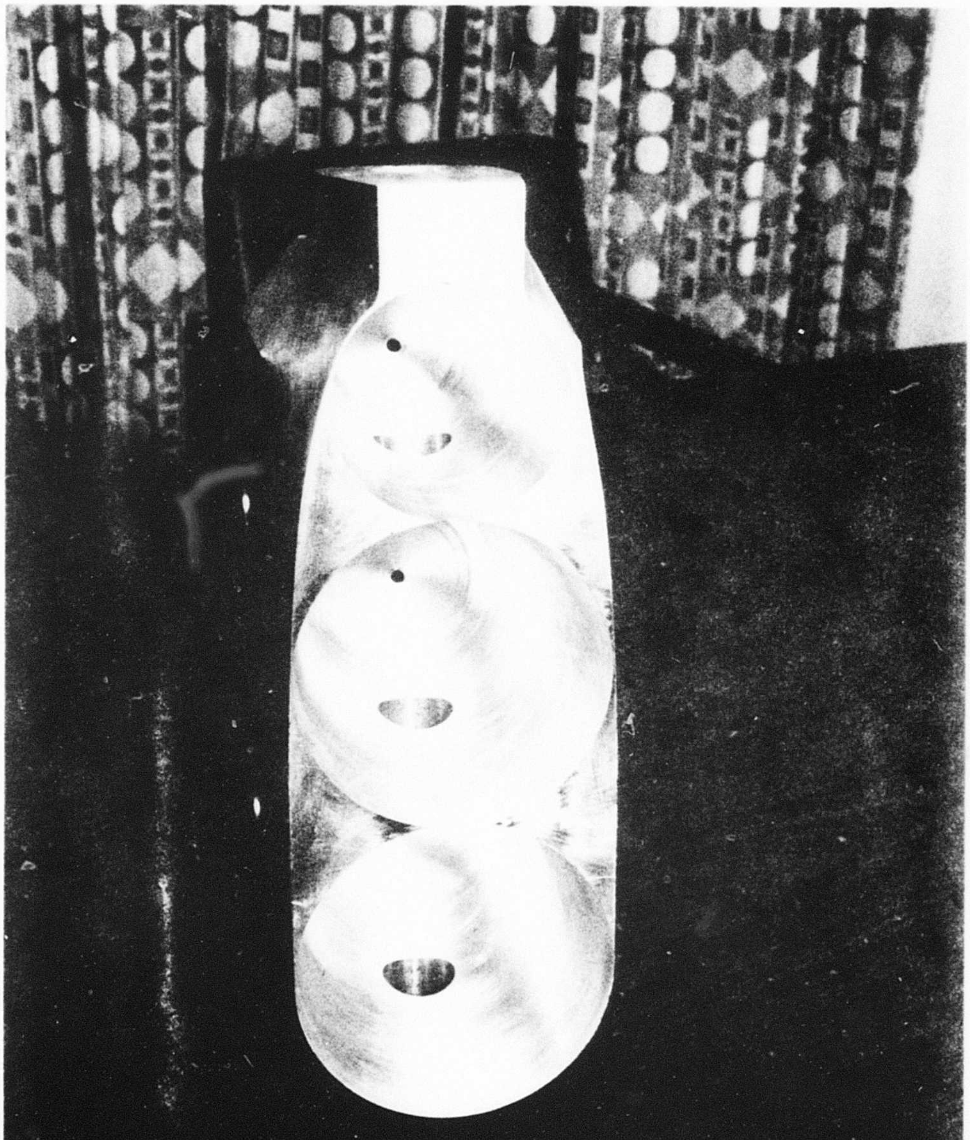

Figure 33. Root end fitting.

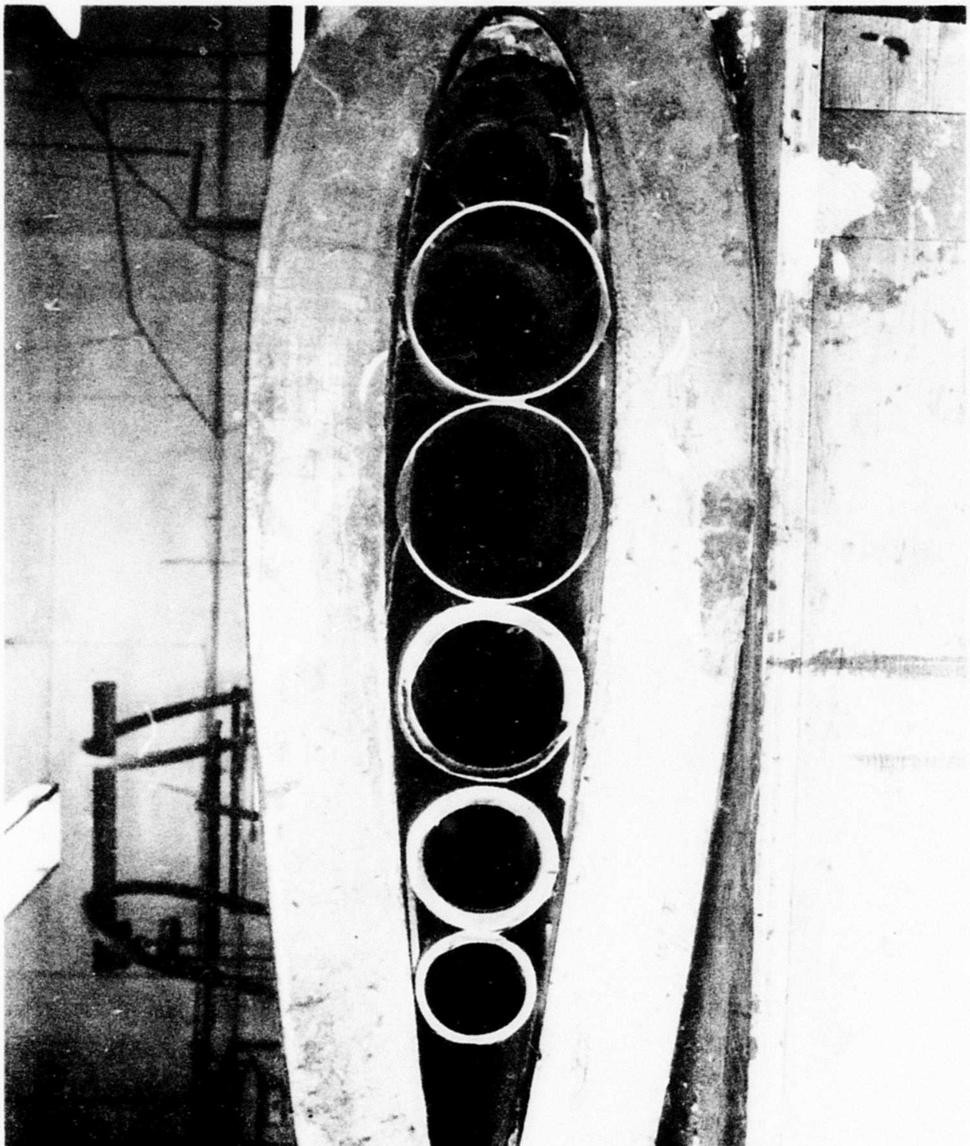

Figure 34. Tubes and longo material supported by the main mold.

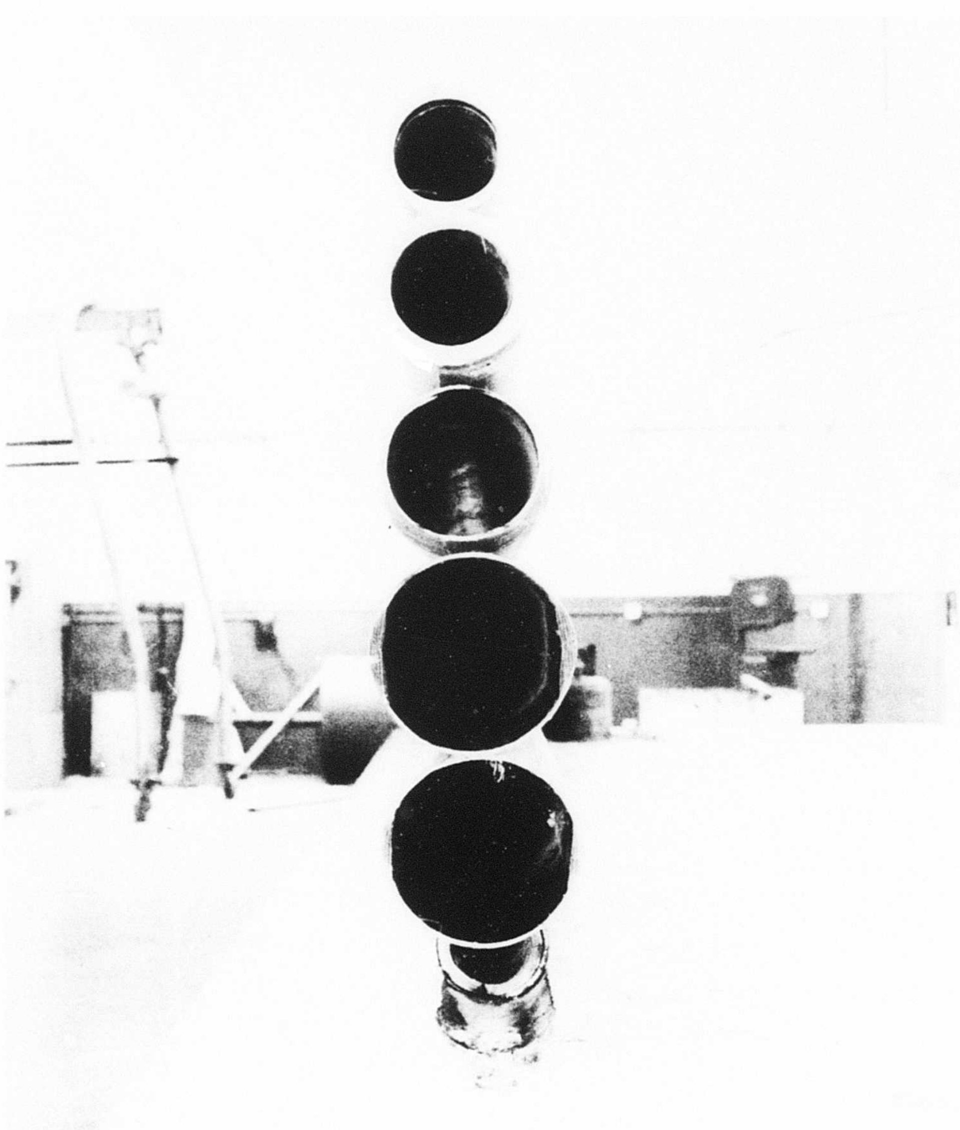

Figure 35. End view of assembled tube and nose longos.

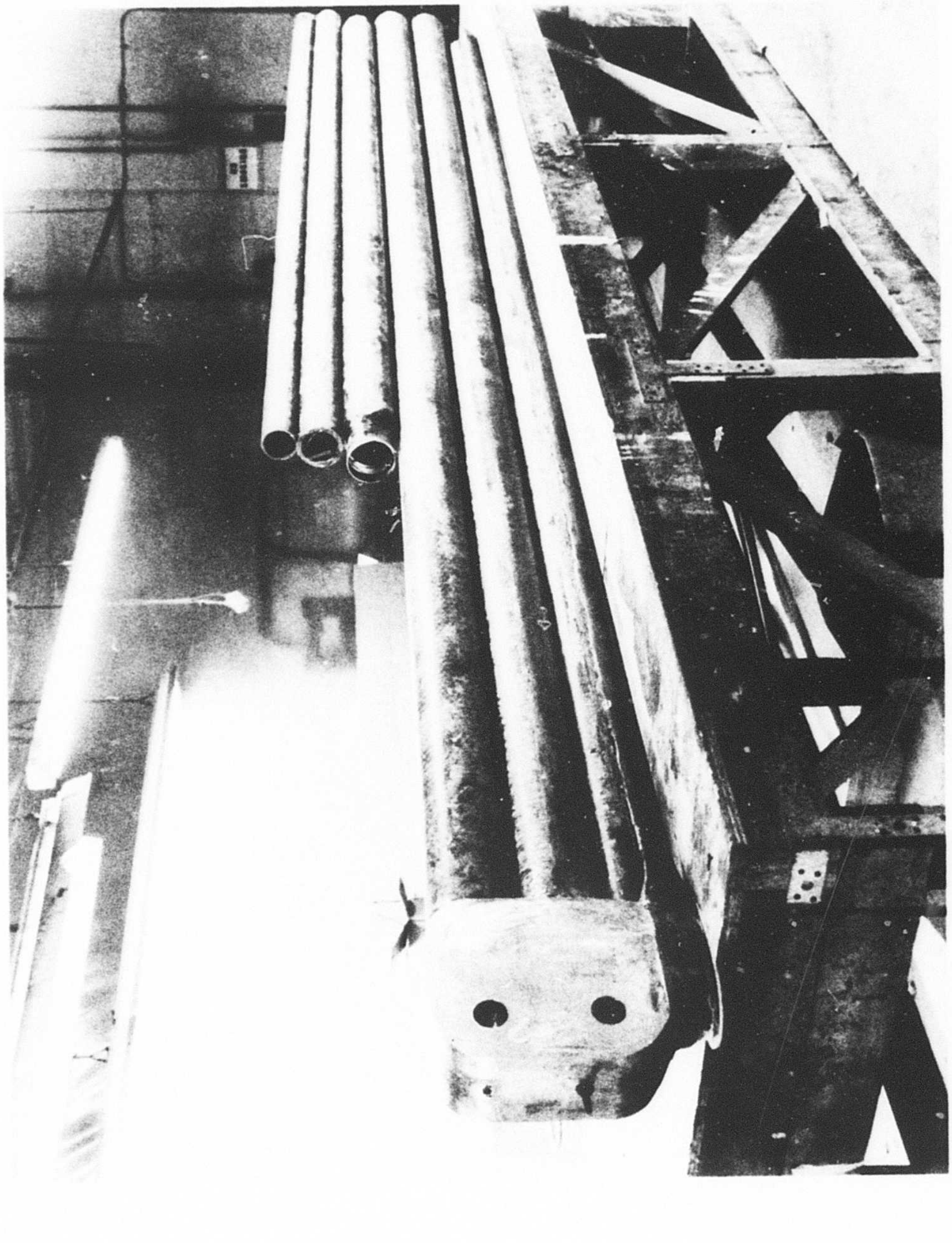

Figure 36. Assembly of tubes, nose longos, and root end fitting.

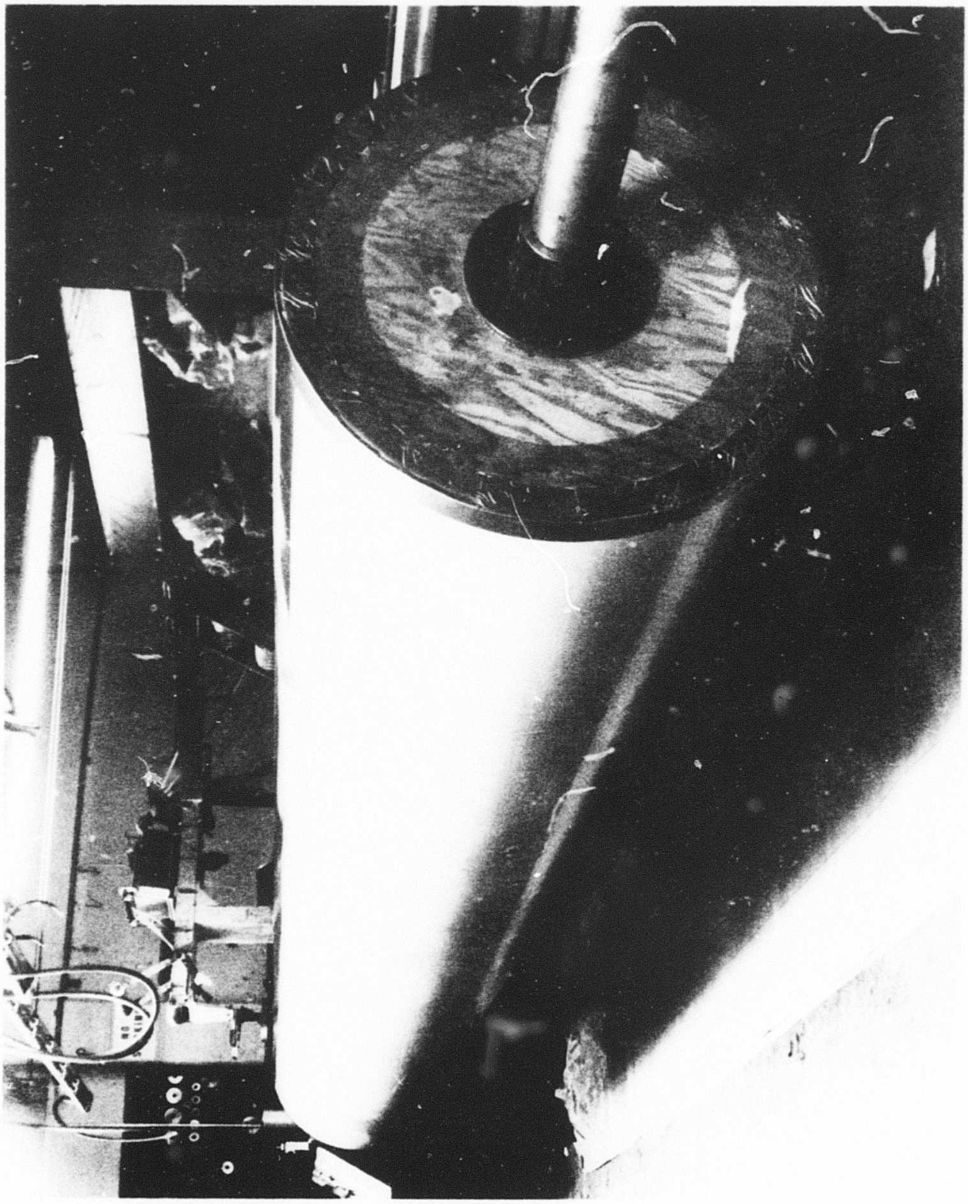

Figure 37. Skin mandrel.

Figure 38. Support structure built inside the skin mandrel.

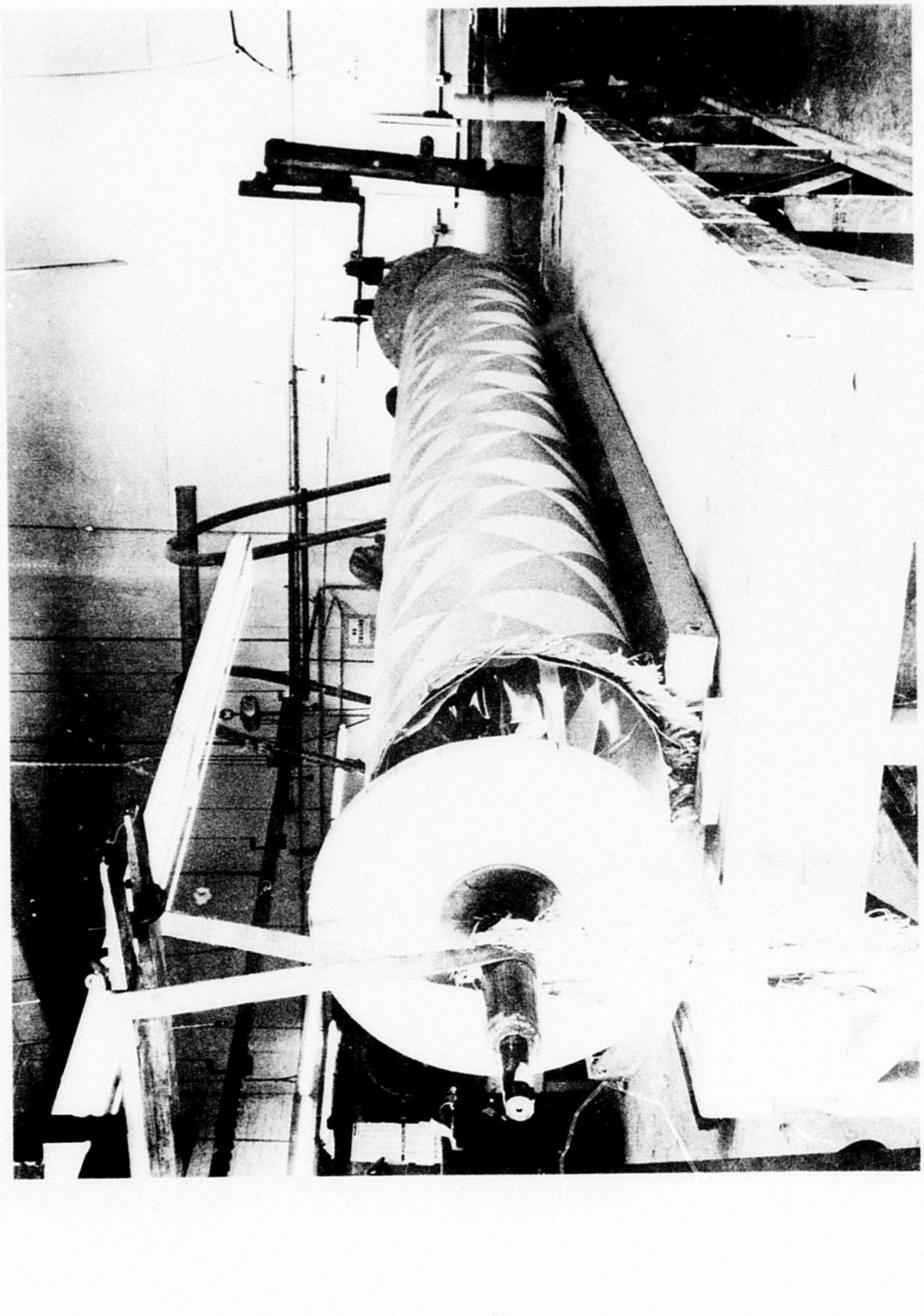

Figure 39. Skin material being placed in mold.

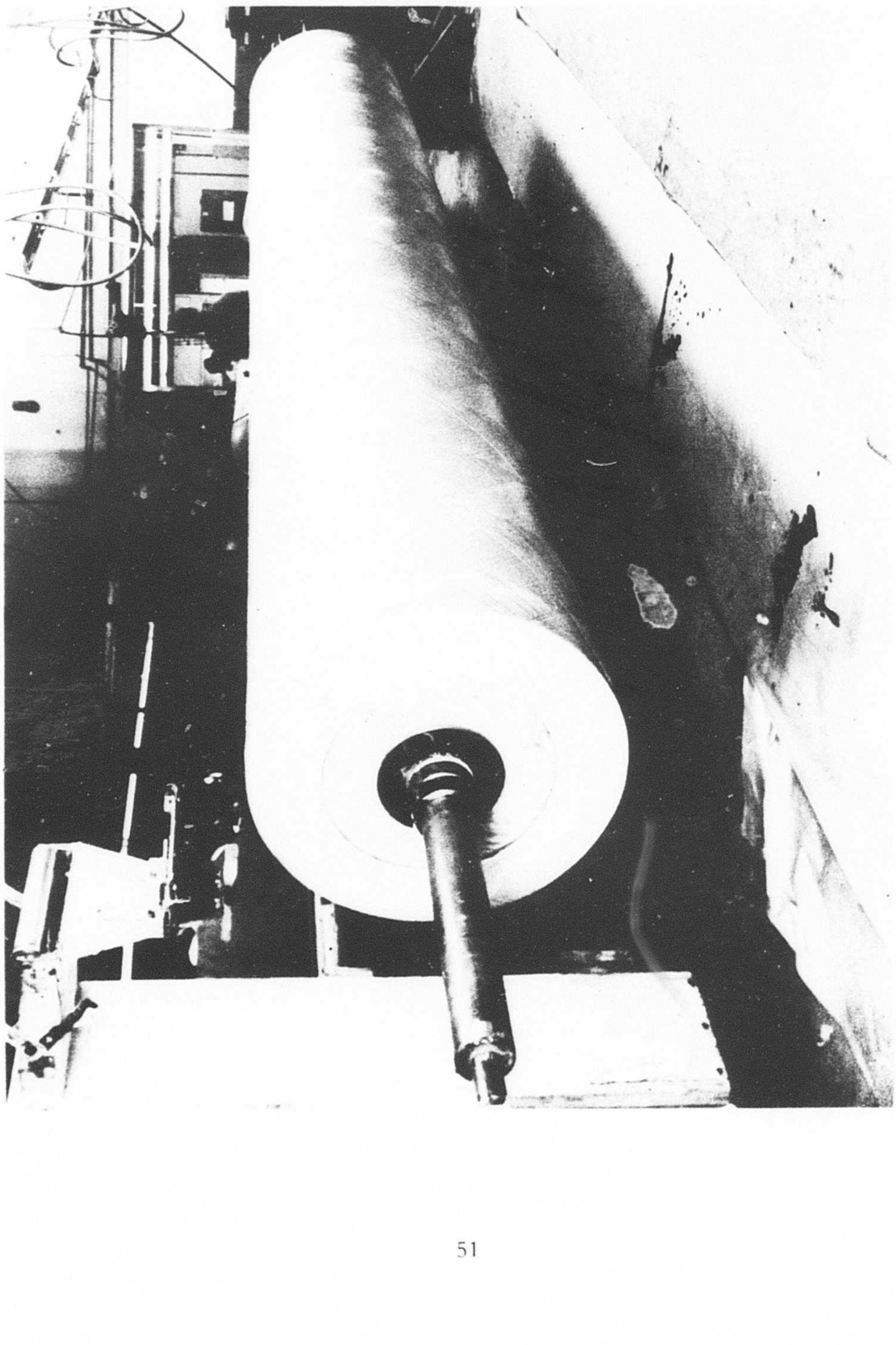

Figure 40. Wound skin material.

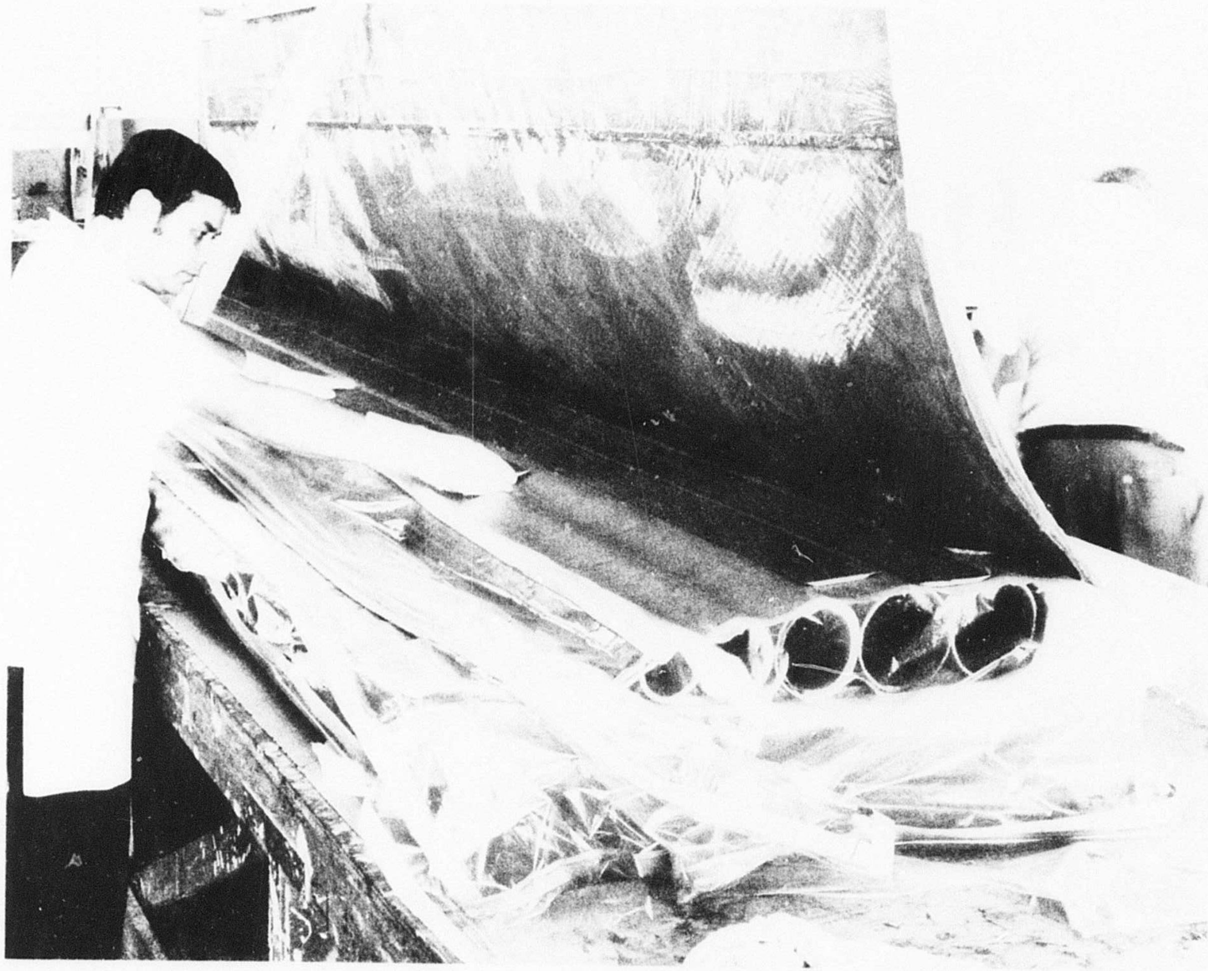

Figure 41. Layup of inside skin and core material.

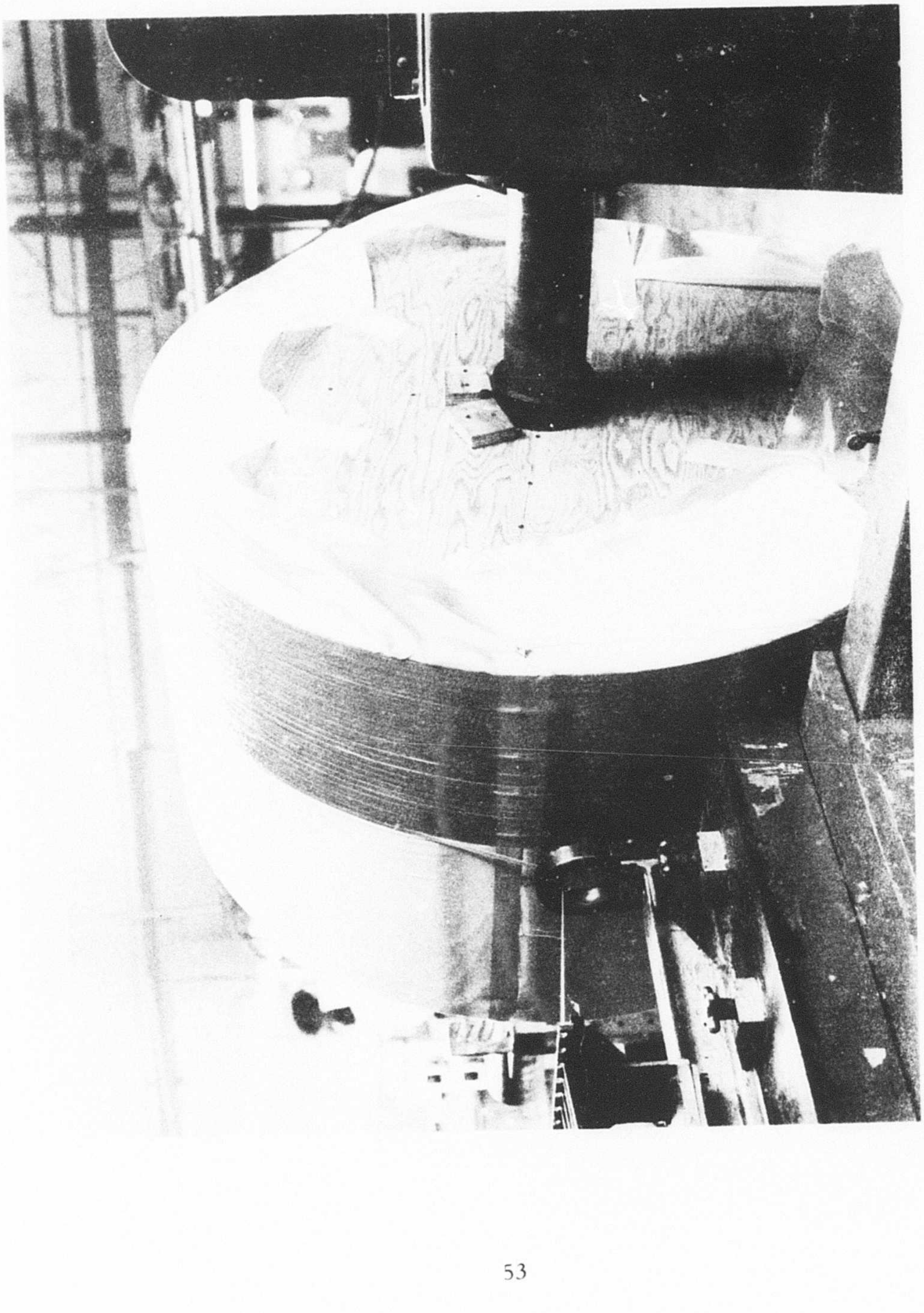

Figure 42. Winding of longo doubler material.

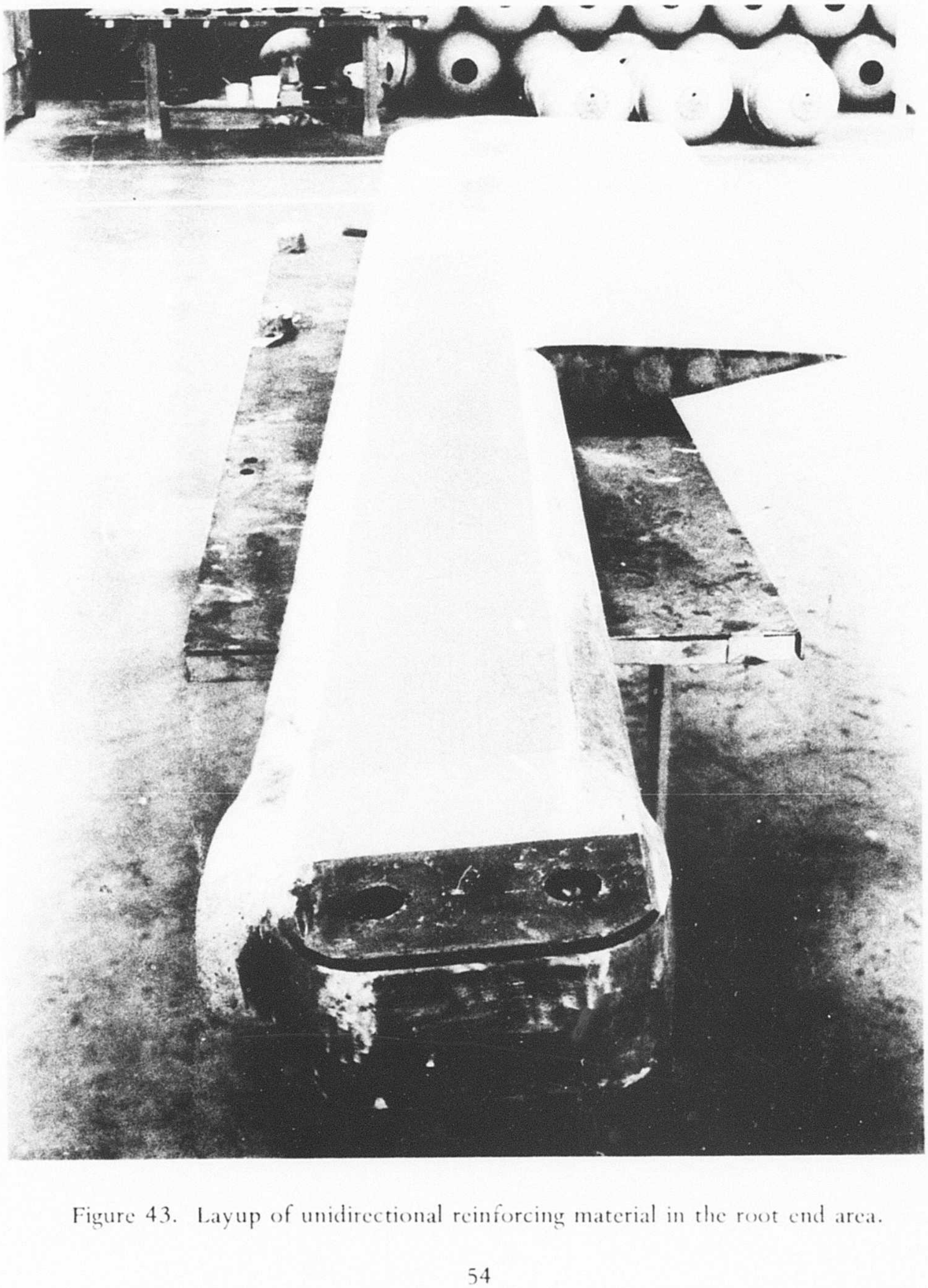

Figure 43. Layup of unidirectional reinforcing material in the root end area.

TABLE 1. BLADE CROSS-SECTIONAL PROPERTY SUMMARY

Property	Criteria	Design
W, lb/in.	1.60	1.57
CG, in.	10.44	10.34
EA, 10^6 lb.	112	116
EIX, 10^6 lb-in.^{2}	385	415
EIY, 10^6 lb-in.^{2}	9000	10581
GJ, 10^6 lb-in.^{2}	255	280

TABLE 2. ROTOR BLADE PROPERTIES, MATERIAL WEIGHT, AND MATERIAL COSTS (STATION 138.00)

	Properties									Material weight (lb/in.)						
Design	W (lb/in.)	CG (in.)	NA (in.)	EA (10^6 lb)	EIX (10^6 lb-in.^{2})	EIY (10^6 lb-in.^{2})	GJ (10^6 lb-in.^{2})	Skin material	Tube longo material	S-1014	PRD-49	T-300	T-50S	T-75S	Ceramic	Material Cost/In.*
Criteria	1.60	10.44	-	112.0	385.0	9,000.0	255.0									
1	1.57	10.83	9.28	112.6	396.0	11,282.0	243.4	PRD-49 $\alpha = 31^\circ$	PRD-49	1.0476	.5240					$10.20
2	1.62	10.40	8.99	121.3	407.9	12,296.0	244.3	PRD-49 $\alpha = 31^\circ$	PRD-49	1.0931	.5231					10.34
3	1.59	10.46	8.98	132.0	511.7	11,004.0	172.3	S-Glass $\alpha = 40^\circ$	T-300	1.4439		.1495				9.71
4	1.61	10.60	8.36	101.3	309.6	10,042.0	169.1	S-Glass $\alpha = 40^\circ$	S Glass	1.6085						5.20
5	1.56	10.21	9.61	124.4	426.8	14,498.0	265.3	T-300 $\alpha = 30^\circ$	PRD-49	1.1037	1459	.3099				15.92
6	1.51	10.18	9.55	125.5	435.3	14,485.0	265.3	T-300 $\alpha = 30^\circ$	T-300	1.1037		.4038				17.19
6A	1.44	10.48	9.73	122.0	432.5	14,523.0	262.1	T-300 $\alpha = 30^\circ$	T-300	1.0399		.4042				17.00
7	1.67	10.30	8.69	94.8	302.2	11,846.0	186.4	S-Glass $\alpha = 45^\circ$	S-Glass	1.1573					.5085	12.66
8	1.47	10.38	10.31	175.1	795.8	15,585.0	371.4	T-50S $\alpha = 30^\circ$	T-50S	1.0399			.4315			56.55
9	1.49	10.45	10.66	212.6	1,036.2	17,462.0	476.5	T-75S $\alpha = 30^\circ$	T-75S	1.0399				.4506		80.59
10	1.56	10.07	9.35	136.8	555.1	14,321.0	227.8	PRD-49 $\alpha = 32^\circ$	T-300	.5413	.3388	.1818			.4961	20.34
11	1.43	10.28	9.54	104.1	394.1	12,591.0	255.7	PRD-49 $\alpha = 40^\circ$	T-300	.5413	.3388	.1040			.4961	17.72
12	1.54	10.45	9.06	115.0	414.6	10,527.0	277.7	PRD-49 $\alpha = 40^\circ$	T-300	1.0931	.3388	.1040				11.45
12A	1.57	10.34	9.01	116.4	415.0	10,581.0	280.0	PRD-49 $\alpha = 40^\circ$	T-300	1.1257	.3388	.1040				11.55

*Cost = $ 3.23 - S-1014
13.01 - PRD-49
33.75 - T-300
123.27 - T-50S
171.40 - T-75S
17.55 - Ceramic

TABLE 3. FIBER PROPERTY AND COST SUMMARY

Property	S-1014	Kevlar 49	Thornel 300	Thornel 400	Thornel 50S	Thornel 75S
ρ, lb/in.^{3}	.0900	.0524	.0614	.0643	.0600	.0660
<u>Axial</u>						
F_{tu}, psi	325,000	400,000	325,000	425,000	285,000	345,000
E, 10^6 psi	12.6	19.0	34.0	30.0	57.0	79.0
ϵ, %	3.0	2.0	1.0	1.3	0.6	
α, 10^{-6}in./in./°F	2.2	−3.44			−.24	−.24
μ	.22					
<u>Radial</u>						
F_{tu}, psi						
E, 10^6 psi	12.6	1.42	1.3	1.2	1.1	1.0
G, 10^6 psi	5.17	0.27	3.5	3.5	3.5	3.5
α, 10^{-6}in./in./°F	2.2				2.96	2.96
μ	.22					
<u>Cost</u>						
$/lb	4.10	22.00	55.00	205.00	205.00	275.00
$/in.^{3}	0.369	1.153	3.377	13.181	12.300	18.150

TABLE 4. HIGH-DENSITY (CERAMIC) FIBER PROPERTY AND COST SUMMARY

Type*	Sp. Gr. Gm/cc	Density lb /in.^{3}	Modulus 10^6 psi.	Strength psi	Cost $/lb	Cost $/in.^{3}
2	2.6	.0939	23-25	200,000	7.50	0.704
10	3.8	.1373	14	200,000	7.50	1.030
15	4.6	.1662	15	-	15.00	2.493
16	5.7	.2059	16	-	15.00	3.088
17	7.4	.2674	18	-	20.00	5.348
20	8.1	.2926	-	-	25.00	7.315

* Product of 3M Company (Still in research stage).

TABLE 5. MAXIMUM STRESS AND PERCENTAGE OF SINGLE-CYCLE STRENGTH (LIMIT LOADS)

Number	Skin		Tube Longos	
	σ	% S. C. S.	σ	% S. C. S.
1	8,639	24.0	30,873	17.2
2	8,190	22.8	29,174	16.2
3	5,747	10.8	43,845	40.5
4	8,372	15.7	24,570	15.1
5	16,060	55.4	28,190	15.7
6	15,834	54.6	49,174	45.4
6A	16,127	55.6	50,093	46.2
7	7,249	17.3	25,724	15.8
8	10,353	35.7*	52,352	48.4*
9	10,523	36.3*	58,028	53.6*
10	6,053	17.8	42,093	38.9
11	3,893	19.0	57,008	52.7
12	3,602	17.5	52,728	48.7
12A	3,576	17.4	52,296	48.3

* Thornel 300 strength properties used.

TABLE 6. COMPONENT DESIGN

Outside Skin (Kevlar 49/epoxy)

$\alpha = \pm 40^{o}$

$V_f = .50$

$E_x = 1.163 \times 10^6$ psi

$E_y = 0.703 \times 10^6$ psi

$G = 2.439 \times 10^6$ psi

$F_x = 23,083$ psi

$F_y = 12,150$ psi

$F_{xy} = 10,000$ psi (Approximation)

$\rho = .0463$ lb/in.^{3}

Inside Skin (Style 1557 "E" Glass Fabric/Epoxy)

$V_f = .50$

$E_x = .785 \times 10^6$ psi

$E_y = 4.480 \times 10^6$ psi

$G = 1.600 \times 10^6$ psi

$F_x = 13,100$ psi

$F_y = 74,700$ psi

$F_{xy} = 8,000$ psi

$\rho = .0661$ lb/in.^{3}

Nose Longos (S-Glass/Epoxy)

$\alpha = 0^{o}$

$V_f = .50$

$E_x = 6.550 \times 10^6$ psi

$E_y = 1.922 \times 10^6$ psi

$G = 0.564 \times 10^6$ psi

$F_x = 168,000$ psi

$\rho = .0651$ lb/in.^{3}

Tubes No. 1, 2, and 3 (S-Glass/Epoxy)

20% at $\alpha = 90^{o}$

80% at $\alpha = \pm 30^{o}$

$V_f = .58$

$E_x = 3.974 \times 10^6$ psi

$E_y = 3.056 \times 10^6$ psi

$G = 1.582 \times 10^6$ psi

$F_x = 91,400$ psi

$F_y = 55,100$ psi

$F_{xy} = 16,500$ psi

$\rho = .0691$ lb/in.^{3}

TABLE 6. CONTINUED

Longos Tubes No. 2 and 3 (Thornel 300/Epoxy)

$\alpha = 0^{o}$

$V_f = .50$

$E_x = 17.25 \times 10^6$ psi

$F_x = 108{,}300$ psi

$\rho = .0508$ lb/in.^{3}

Outside Face Tubes No. 4, 5, and 6 (S-Glass/Epoxy)

50% at $\alpha = \pm 30^{o}$

50% at $\alpha = 90^{o}$

$V_f = .58$

$E_x = 3.493 \times 10^6$ psi

$E_y = 4.732 \times 10^6$ psi

$G = 1.243 \times 10^6$ psi

$F_x = 59{,}600$ psi

$F_y^{\bullet} = 106{,}900$ psi

$F_{xy} = 13{,}300$ psi

$\rho = .0715$ lb/in.^{3}

Inside Face Tubes No. 4, 5, and 6 (S-Glass/Epoxy)

100% at $\alpha = 90^{o}$

$V_f = .58$

$E_y = 7.518 \times 10^6$ psi

$\rho = .0691$ lb/in.^{3}

PVC Foam Core

Rigicell 400		Rigicell 500	
E_c	= 4500 psi	E	= 6000 psi
G	= 3500 psi	G	= 4500 psi
F_{cu}	= 140 psi	F_{cu}	= 210 psi
F_{su}	= 100 psi	F_{su}	= 140 psi
ρ	= .002315 lb/in.^{3}	ρ	= .002894 lb /in.^{3}

Epoxy Resin (Applied Plastic Company 2434/2345)

$E = .50 \times 10^6$ psi

$F_{tu} = 11{,}000$ psi

$\rho = .0402$ lb/in.^{3}

Cure cycle: 4 hours at 130°F + 2 hours at 180°F + 2 hours at 250°F.

TABLE 7. TUBULAR COMPOSITE ROTOR BLADE CROSS-SECTIONAL PROPERTIES – COMPUTER OUTPUT

ROTOR BLADE SKIN CROSS-SECTION PROPERTIES

N	XO	YO	TS	XI	YI	RHOS	ES	GS
1	0.0000	0.0000	.0600	.0600	0.0000	.0687	1.163E+06	2.489E+06
2	.2500	.6801	.0600	.2500	.5516	.0687	1.163E+06	2.489E+06
3	.5000	.9470	.0600	.5000	.8651	.0687	1.163E+06	2.489E+06
4	.7500	1.1451	.0600	.7500	1.0711	.0687	1.163E+06	2.489E+06
5	1.0000	1.3074	.0600	1.0000	1.2385	.0687	1.163E+06	2.489E+06
6	1.5000	1.5687	.0600	1.5000	1.5024	.0687	1.163E+06	2.489E+06
7	2.0000	1.7773	.0600	2.0000	1.7131	.0687	1.163E+06	2.489E+06
8	2.5000	1.9513	.0600	2.5000	1.8883	.0687	1.163E+06	2.489E+06
9	3.0000	2.1000	.0600	3.0000	2.0376	.0687	1.163E+06	2.489E+06
10	3.3300	2.1859	.0600	3.3300	2.1242	.0687	1.163E+06	2.489E+06
11	4.0000	2.3414	.0600	4.0000	2.2804	.0687	1.163E+06	2.489E+06
12	6.0000	2.6726	.0600	6.0000	2.6122	.0687	1.163E+06	2.489E+06
13	9.0000	2.9298	.0600	9.0000	2.8697	.0687	1.163E+06	2.489E+06
14	12.0000	3.0009	.0600	12.0000	2.9409	.0687	1.163E+06	2.489E+06
15	16.0000	2.9012	.0600	16.0000	2.8411	.0687	1.163E+06	2.489E+06
16	20.0000	2.6470	.0600	20.0000	2.5868	.0687	1.163E+06	2.489E+06
17	25.0000	2.1764	.0600	25.0000	2.1161	.0687	1.163E+06	2.489E+06
18	30.0000	1.5802	.0600	30.0000	1.5197	.0687	1.163E+06	2.489E+06
19	35.0000	.8773	.0600	35.0000	.8166	.0687	1.163E+06	2.489E+06
20	40.0000	.0630	.0600	40.0000	0.0000	.0687	1.163E+06	2.489E+06

W = .3388
CG = 19.7039
A = 161.013
L = 82.133
AS = 4.9320
J = 75.7553
EA = 5.7359E+06
EIX = 2.6813E+07
GJ = 1.8856E+08

TABLE 7. Continued

ROTOR BLADE TUBE CROSS-SECTION PROPERTIES

N	RO	RI	T	X	E	G	RHO
1	2.0328	1.3828	.6500	3.3062	3.9740E+06	1.5820E+06	.0691
2	2.8010	2.6760	.1250	8.1400	3.9740E+06	1.5820E+06	.0691
3	2.9070	2.7820	.1250	13.8480	3.9740E+06	1.5820E+06	.0691
4	2.8170	2.1666	.6504	19.3720	1.0330E+05	3.6740E+04	.0062
5	2.1630	1.6376	.5254	24.3520	1.2730E+06	4.5300E+04	.0070
6	1.7200	1.4448	.2754	28.2350	2.3090E+05	8.2200E+04	.0106

N	A	W	I	EA	EIX	GJ
1	6.9748	.4820	10.5396	2.7718E+07	4.1884E+07	3.3347E+07
2	2.1508	.1486	8.0691	8.5478E+06	3.2067E+07	2.5531E+07
3	2.2341	.1544	9.0425	8.8782E+06	3.5935E+07	2.8610E+07
4	10.1829	.0631	32.1517	1.0519E+06	3.3213E+06	2.3625E+06
5	6.2732	.0439	11.5432	7.9858E+06	1.4695E+07	1.0458E+06
6	2.7380	.0290	3.4535	6.3220E+05	7.9741E+05	5.6775E+05

W = .9210
CG = 8.7434
AT = 30.5538
EA = 5.4813E+07
EIX = 1.2870E+08
GJ = 9.1464E+07

ROTOR BLADE TUBE LONGO PROPERTIES

N	A	W	EA	EIX	N	RI	H	RHO	EI
1	0.0000	-0.0000	-0.	0.	1	1.3828	1.3828	-0.0000	-0.
2	.5456	.0277	9.4109E+06	6.3683E+07	2	2.6760	2.4760	.0508	1.7250E+07
3	1.4994	.0762	2.5864E+07	1.7965E+08	3	2.7820	2.3920	.0508	1.7250E+07
4	0,0000	-0.0000	-0.	0.	4	2.1666	2.1666	-0.0000	-0.
5	0.0000	-0.0000	-0.	0.	5	1.6376	1.6376	-0.0000	-0.
6	0.0000	-0.0000	-0.	0.	6	1.4446	1.4446	-0.0000	-0.

W = .1039
CG = 12.3252
EA = 3.5275E+07
EIX = 2.4333E+08

LIST OF SYMBOLS

A	Area (in.^{2}), angle (deg)
AS	Skin cross-sectional area (in.^{2})
AT	Tube cross-sectional area (in.^{2})
C	Dimension (in.), chord length (in.)
CF	Centrifugal force (lb)
CG	Distance from blade leading edge to center of gravity (in.)
E	Modulus of elasticity (psi)
EA	Spanwise stiffness (lb)
ES	Spanwise modulus of elasticity of skin material (psi)
EIX	Flapping bending stiffness (lb-in.^{2})
EIY	Chordwise bending stiffness (lb-in.^{2})
F	Allowable strength (psi)
G	Shear modulus of elasticity (psi)
GJ	Torsional stiffness (lb-in.^{2})
GS	Shear modulus of elasticity of skin material (psi)
H	Dimension from tube center to flats (in.)
I	Moment of inertia (in.^{4})
J	Torsional constant (in.^{4})
L	Mean skin perimeter (in.)
N	Number
NA	Distance from leading edge to neutral axis chordwise bending (in.)
R	Radius (in.)

RI	Inside tube radius (in.)
RO	Outside tube radius (in.)
RHO	Density ($lb/in.^3$)
RHOS	Equivalent density of skin material ($lb/in.^3$)
SCS	Single cycle strength
SF	Dimension from leading edge to end of nose longo material (in.)
T	Thickness (in.)
TS	Thickness of blade skin material (in.)
V	Volume ratio
W	Unit weight (lb/in.), width (in.)
X	Dimension (in.)
XI	Inside dimension (in.)
XO	Outside dimension (in.)
YI	Inside dimension (in.)
YO	Outside dimension (in.)
α	Winding angle (deg), coefficient of thermal expansion ($in./in./^{\circ}F$)
ϵ	Elongation (in./in.)
u	Poisson's ratio
ρ	Density ($lb/in.^3$)
σ	Unit stress (psi)

Subscripts

c	Denotes compression
f	Refers to fibers

su	Denotes shear ultimate
tu	Denotes tension ultimate
y	Denotes chordwise direction
x	Denotes spanwise direction

12680-74